Bioorganic Chemistry 88 (2019) 102899

Contents lists available at ScienceDirect

Bioorganic Chemistry

journal homepage: www.elsevier.com/locate/bioorg

Synthesis and identification of quinoline derivatives as topoisomerase I inhibitors with potent antipsoriasis activity in an animal model

Wen-Jin Zhang[a,1], Peng-Hui Li[a,b,1], Min-Cong Zhao[a], Yao-Hao Gu[a], Chang-Zhi Dong[a,c], Hui-Xiong Chen[a,d], Zhi-Yun Du[a,*]

[a] Institute of Natural Medicine & Green Chemistry, School of Chemical Engineering and Light Industry, Guandong University of Technology, Guangzhou 510006, China
[b] School of Life Science, Huizhou University, Huizhou 516001, China
[c] Universite Paris Diderot, Sorbonne Paris Cite, ITODYS, UMR 7086 CNRS, 15 rue J-A de Baif, 75270 Pairs Cedex 13, France
[d] CNRS, UMR8601, Laboratoire de Chimine et Biochimie Pharmacologiques et Toxicologiques, CBNIT, Universite Paris Descartes PRES Sorbonne Paris Cite, UFR Biomedicale, 45 rue des Saints-Peres, 75270 Paris Cedex 06, France

ARTICLE INFO

Keywords:
Psoriasis
Topoisomerase I
Quinoline derivatives
Proinflammatory markers
Imiquimod-induced inflammation

ABSTRACT

Psoriasis is a chronic inflammatory and immune-mediated skin disease. Although certain agents have shown clinical success in treating psoriasis, development of safe and effective strategies for the treatment of this condition remains important. Research suggests that DNA topoisomerase I (Topo I) inhibitors may have potent psoriasis-ameliorating effects. Here, 25 quinoline derivatives were synthesized and identified as Topo I inhibitors. These compounds inhibited the 12–*O*–tetradecanoylphorbol-13-acetate-induced mouse ear inflammation. The most potent analogs, **5i** and **5l**, suppressed the expression of inflammatory cytokines in lipopolysaccharide-stimulated HaCaT cells. Additionally, the lead compounds significantly improved imiquimod-induced psoriasis-like inflammation in mice. Moreover, the expression levels of cytokines and inflammatory mediators, such as interleukin (IL)-17A, IL-22, IL-23, nuclear factor-κB subunit p65, tumor necrosis factor-α, and interferon-γ, were dramatically inhibited in the dorsal skin of **5i**- and **5l**-treated mice. These findings indicate that the inhibition of Topo I activity may potentially be an effective strategy for psoriasis treatment.

1. Introduction

Psoriasis is a chronic inflammatory and immune-mediated skin disease characterized by hyperproliferation and poor differentiation of keratinocytes [1–3]. Psoriasis has prevalence ranging from 0.2% to 4.8%, and associated with economic and clinical factors and significantly affects the patient's quality of life [4]. The mechanism of pathogenesis has been thoroughly investigated for psoriasis in the last three decades, and significant evidence indicates that the immune response, secreted factors, and cellular mediators play important roles in the development and maintenance of psoriasis [5–7]. Moreover, studies have suggested that many cytokines and inflammatory mediators, such as nuclear factor (NF)-κB, interleukin (IL)-22, IL-6, IL-17, IL-23, interferon (IFN)-γ, and tumor necrosis factor (TNF)-α, are involved and interact as a network in the pathogenesis of psoriasis [8–10]. Currently, the main approaches to the treatment of psoriasis include systemic antiproliferative or immunosuppressive agents, such as vitamin D analogs, methotrexate, and acitretin, as well as biological agents (e.g., etanercept, ustekinumab, and ixekizumab) [11–15]. These drugs are often effective for moderate to severe psoriasis. However, most of them cause considerable toxicity and side effects, and a long duration of treatment is needed [2,16,17]. Although the drugs usually have strong effects in early treatment, they cannot be used in long term because of immune deregulation [18]. More seriously, once the treatment is stopped, patients may experience more severe symptoms [19]. Hence, it is urgent to develop safe and effective strategies for the treatment of psoriasis [1,20].

DNA topoisomerase I (Topo I) is a nuclear enzyme essential for resolving topological problems that occur during DNA transcription, replication, and chromosome segregation [21]. Topo I plays a critical role in cell proliferation and is considered as important target for the prevention of rapid proliferation of cancer cells [22]. Several Topo I inhibitors have been widely used in the clinic for decades not only as anticancer drugs, but also for their curative effects on psoriasis [23]. For instance, camptothecin (CPT, Fig. 1) has exhibited a significant curative efficacy in the treatment of psoriasis [24]. Lin et al. [25] have

* Corresponding author.
E-mail address: zhiyundu@gdut.edu.cn (Z.-Y. Du).
[1] These authors contributed equally to this work.

https://doi.org/10.1016/j.bioorg.2019.03.073
Received 18 January 2019; Received in revised form 26 February 2019; Accepted 30 March 2019
Available online 04 April 2019

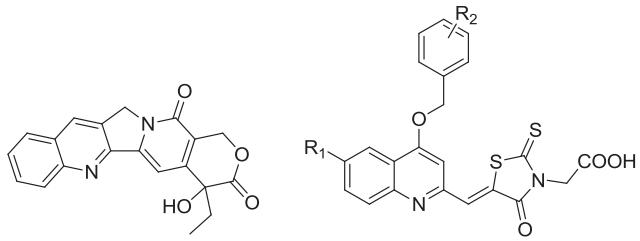

Fig. 1. Structures of CPT and quinoline derivatives.

subsequently revealed that CPT and isoCPT inhibited the growth of cultured normal human adult keratinocytes in vitro by inducing apoptosis. Their further results have demonstrated that the therapeutic mechanism of CPT against psoriasis may be associated with its anti-proliferative activity and the apoptosis of keratinocytes may be mediated through downregulation of telomerase activity [26,27]. Marazzi et al. [28] have found that chemical inhibition of Topo I suppressed the expression of proinflammatory cytokines (e.g., IL-6, IL-8, and TNF-α) and inhibited the endogenous expression of two key pathogen-associated molecular pattern-induced genes, namely, those encoding IFN-β and IFIT1 (IFN-induced protein with tetratricopeptide repeats 1). Taken together, Topo I is likely involved in psoriasis and represents a potential molecular target for the treatment of psoriasis.

The imiquimod (IMQ)-induced psoriasis-like BALB/c mouse model, whose characteristics resemble most of the features of clinical psoriasis, has been widely used in studies of psoriasis. Topical application of a 5% IMQ cream on mouse skin could lead to hyperkeratosis and scaling of the skin, mimicking the typical symptoms associated with psoriasis [29]. Furthermore, the IMQ model resembles human psoriatic inflammation in many aspects, one of them being a major involvement of the IL-23/IL-17A/IL-22 axis. This has been confirmed by the efficacy of anti-IL23, anti-IL-17A, and anti-IL-22 antibodies in mouse psoriasis-like skin inflammation models and anti-IL23/IL-17A antibodies in human psoriatic patients [30–32].

Quinoline is widely used in the drug design and discovery to develop bioactive molecules with various pharmacological activities, such as antimalarial, antibiotic, antitumor, and anti-inflammatory activities [33–35]. In this study, a series of quinoline derivatives (QCs, Fig. 1) were synthesized and identified as potent Topo I inhibitors and anti-inflammatory agents. The most active compounds were evaluated for their antipsoriatic effects by employing lipopolysaccharide (LPS)-stimulated HaCaT cells and the IMQ-induced psoriasis-like mouse model. A further study in the mouse model showed that the leading compounds exhibited strong effects on the expression of key cytokines associated with psoriasis. The results revealed that QCs functioned as potential antipsoriasis agents.

2. Results and discussion

2.1. Chemistry

The synthesis of 25 QCs was accomplished as outlined in Scheme 1. Various anilines (**1a–1g**) were treated with ethyl acetoacetate in the presence of polyphosphoric acid to obtain the corresponding QCs (**2a–2g**) [36]. Compounds **2a–2g** were treated with appropriate benzyl bromides using KOH as the base to obtain **3a–3v** in 63–76% yields. Compounds **3a–3v** were oxidized by SeO_2 to obtain **4a–4v** in 68–85% yields. The target compounds **5a-5y** were finally synthesized in 71–88% yields through the Hornor–Wadsworth–Emmons reaction [37] of the rhodanine moiety with the prepared aldehydes (**4a–4v**). The structures of QCs were characterized and confirmed by ^{1}H NMR and ^{13}C NMR.

2.2. QCs as potent Topo I inhibitors

Topo I-mediated supercoiled pBR322 DNA plasmid relaxation assay was first carried out to evaluate the inhibitory activities of QCs against Topo I [38]. Compound **5a-5o** with different substitutions on the phenyl ring were first synthesized and evaluated. The results, presented in Fig. 2, showed that the positive control (CPT) strongly inhibited the Topo I activity. Compound **5a**, **5b**, **5d**, **5e**, **5g**, **5h**, **5n**, **5i** and **5l** displayed potent Topo II inhibition activities at 50 μM (Fig. 2A and Fig. 2B). Among these compounds, **5i** and **5l** displayed the best activity at 20 μM (Fig. 2C). It was found that the substituent in the phenyl ring as well as its position have significant impact on the inhibition of Topo II activity. Compounds **5l**, **5m** and **5n**, which contain a fluorine on phenyl ring, respectively, on the *p*-position (**5l**) displayed better activities than on the ortho (**5m**)- or meta-positions (**5n**). In addition, compounds **5j** and **5k** with two fluorine on phenyl ring have no effect on Topo I inhibition. Compound **5i** with an fluorine on ortho-position and an bromine on *p*-position show much more potency to inhibit Topo I. Compounds **5o-5y** were synthesized on the basis of **5i** and **5l**. However, all of these derivatives exhibited poorer Topo I inhibitory activities than those of **5i** and **5l** (Fig. 2A–C).

2.3. QCs display potent anti-inflammatory activities

Because psoriasis is a chronic inflammatory skin disease, anti-inflammatory activities of QCs were first evaluated in a mouse ear edema model induced by 12–*O*–tetradecanoylphorbol-13-acetate (TPA). [39] Table 1 and Fig. S1 summarize the weights of the ear edema induced by topical TPA treatment in the absence or presence of QCs. Compared to the control group, topically treated with acetone, the average punch weight increased from 7.2 mg to 17.5 mg in the TPA-treated group (Table 1). It was found that the ear weights were significantly lower, from 11.2% to 83.7%, in the QCs (5 μM)-pretreated groups. Among these QCs, **5i** and **5l** significantly inhibited the ear edema formation, by approximately 69.3% and 83.7%, respectively, which was comparable to the effect provoked by CPT (5 μM). In addition, a generally good correlation was observed between the anti-inflammatory and Topo I inhibitory activities of these QCs (Table 1).

Hematoxylin and eosin (H&E) staining was subsequently carried out to study histological changes induced by TPA in the mouse ears [40]. The results of histological assessment are shown in Fig. 3. Histological sections of the ears subjected to topical application of TPA showed significant increases in the dermis thickness and the number of inflammatory cells compared to those in the acetone-treated mice (Fig. 3A and B). Application of CPT, **5i**, and **5l** dramatically suppressed the TPA-induced epidermal hyperplasia and reduced the number of infiltrated inflammatory cells (Fig. 3B).

2.4. QCs inhibit the levels of nitric oxide, IL-17, IL-1β, IL-6, and TNF-α in LPS-stimulated HaCaT cells

Since **5i** and **5l** exhibited the most potent Topo I inhibition and anti-inflammatory activities, these two compounds were selected to investigate whether they could alleviate psoriasis. We first assessed the effects of QCs on HaCaT cells (an immortal cell line derived from human keratinocytes), which are often used to test the effects of drug candidates on psoriasis [41]. To determine the non-toxic concentrations of **5i** and **5l**, cell viability was assessed using the Cell Counting Kit-8 (CCK-8) assay. As shown in Fig. 4A, **5i** and **5l** did not exhibit significant cytotoxicity at the concentration as high as 20 μM. Therefore, we used a concentration of 10 μM for **5i** and **5l** in the following antipsoriasis experiments with cultured HaCaT cells. The HaCaT cells were pretreated with **5i** and **5l** for 4 h, and inflammation was stimulated with LPS. Nitric oxide (NO) is generated by immune-activated cells in inflammation sites and plays a key role in signaling pathways of inflammatory cytokines [42]. Hence, inhibiting the production of NO in

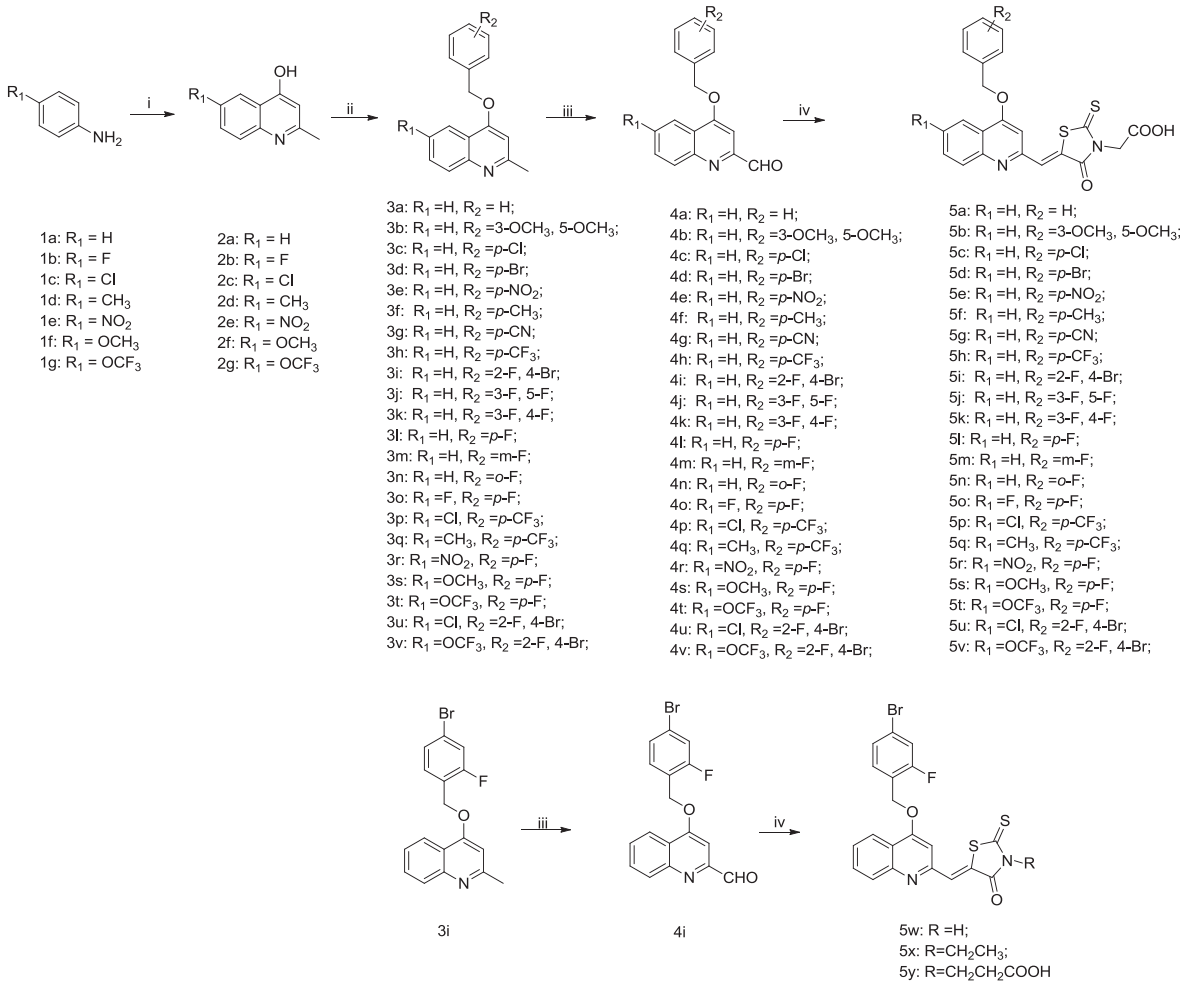

Scheme 1. Synthesis of QCs. Reagents and conditions: (i) PPA, 130 °C, 2 h, (ii) KOH, Me_2O, appropriate benzyl bromide, rt, 8 h, (iii) SeO_2, dioxane, 65 °C, 2 h, (iv) Rhodanine moiety, NaOAc, acetic acid, 110 °C, 4 h.

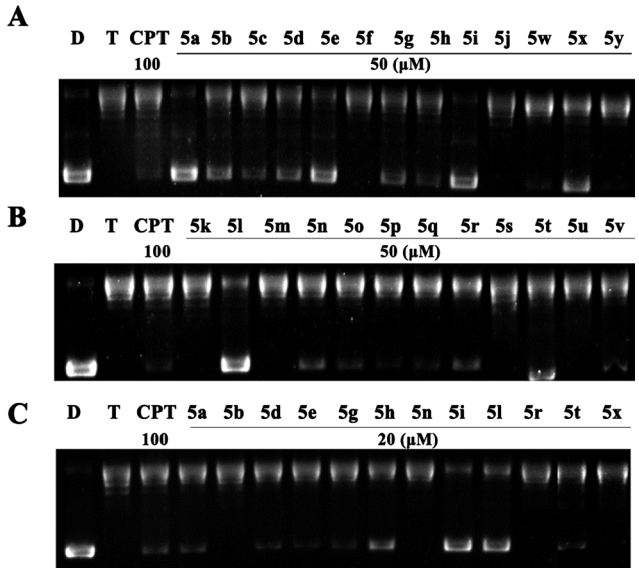

Fig. 2. The Topo I inhibitory activities of QCs. (I, II, and III), lane D, pBR322 DNA, lane T, pBR322 DNA + Topo I, lane CPT, pBR322 DNA + Topo II + CPT (100 μM), other lanes, pBR322 DNA + Topo I + QCs.

the inflammatory response is important. It was found that LPS dramatically increased the level of NO compared with that in the control group. However, treatment with **5i** and **5l** significantly reduced the NO concentration, by 70% and 42% compared to that in the LPS group (Fig. 4B). In further experiments, we examined whether **5i** and **5l** could regulate proinflammatory cytokines such as IL-17A, IL-1β, IL-6, and TNF-α. These cytokines play major roles in maintaining pathogenesis and the course of cutaneous inflammation in psoriasis [43]. As shown in Fig. 4C–F, the mRNA levels of the cytokines significantly increased upon treatment with LPS. However, **5i** and **5l** pretreatment significantly inhibited the expression levels of these cytokines. Taken together, **5i** and **5l** exhibited strong inhibitory effects on the NO production and the expression levels of inflammatory cytokines. These findings indicate that **5i** and **5l** may be potent antipsoriasis agents.

2.5. QCs ameliorate IMQ-induced psoriasis-like skin lesions in mice

The findings showing that **5i** and **5l** could downregulate inflammatory cytokines induced in LPS-stimulated HaCaT cells prompted us to investigate whether these compounds could affect the development of psoriasis. The IMQ-induced psoriasis-like mouse model was employed for this study as previously described [44]. Compounds **5i** and **5l** (50 mg/kg) or CPT (5 mg/kg) were orally administered once daily, followed by application of 62.5 mg of IMQ to the bare skin on the back of mice for seven consecutive days. Compared with that of the

Table 1
Data of inhibition of TPA-induced mice ear edema and Topo I by QCs.

Cpd	Ear weight		Topo I Inhibition[c]	Cpd	Ear weight		Topo I Inhibition
	mg[a]	Inhibition (%)[b]			mg	Inhibition (%)	
Ac	7.2 ± 1.6		n.d.[d]	**5m**	15.4 ± 2.1	23.1	–
Ac/TPA	17.5 ± 1.2		n.d.	**5n**	14.6 ± 1.5	27.6	+
5a	12.6 ± 1.4	47.2	+ +	**5o**	13.9 ± 1.3	35.3	+
5b	13.4 ± 1.1	39.6	+	**5p**	13.7 ± 1.2	37.2	–
5c	14.5 ± 1.7	29.4	+	**5q**	15.2 ± 1.4	22.4	–
5d	12.2 ± 1.0	51.2	+ +	**5r**	14.6 ± 1.7	28.6	+
5e	14.1 ± 1.5	33.4	+	**5s**	15.8 ± 1.7	16.4	–
5f	16.3 ± 1.2	11.2	–	**5t**	13.7 ± 1.2	36.2	+ +
5g	12.5 ± 1.3	48.3	+ +	**5u**	15.1 ± 1.4	23.1	–
5h	13.7 ± 1.3	36.5	+	**5v**	13.6 ± 1.3	37.6	+
5i	8.9 ± 1.1	83.7	+ + +	**5w**	14.4 ± 1.6	29.7	–
5j	15.6 ± 1.4	18.7	–	**5x**	14.3 ± 1.5	30.6	+
5k	15.1 ± 1.3	23.4	–	**5y**	15.8 ± 1.2	16.3	–
5l	10.4 ± 1.2	69.3	+ + +	CPT	10.8 ± 1.3	64.5	+ + +

[a] Each bar represents the mean ± SE from 3 mice.
[b] The inhibitory rate (%) was calculated by this formule: inhibitory rate (%) = (1 − [A(agent group) − B(control group)]/[C(TPA group) − B(control group)]) × 100%.
[c] The relative potent Topo II inhibition of QCs are present as follows: -, no detectable activity at 50 μM, +, weak activity at 50 μM, + +, weak activity at 20 μM, + + +, strong activity at 20 μM.
[d] Not or non-detected.

mice in the control group, the body weight rapidly decreased in the IMQ group, whereas this decline was arrested in the **5i-**, **5l-**, and CPT-treated groups after 3 days of treatment (Fig. S2). The topical results observed after 7 days are shown in Fig. 5A. It was found that the mice in the topical IMQ-treated group did show the development of an apparent psoriasis phenotype, including an erythema, scales, and thickening of the skin. However, the mice, pre-treated with CPT, **5i**, and **5l**, presented much attenuated psoriasis phenotype as there was a gradual reduction in the thickness and scales of skin. The effects were also evident when comparing the reduced grading of Psoriasis Area and Severity Index (PASI, Fig. 5C) scores in CPT, **5i**, and **5l** treatment group with the topical IMQ-treated group. These results suggest that **5i** and **5l** may be of potential value for improving psoriasis-like symptoms in the skin.

To confirm the protective effects of **5i** and **5l** on IMQ-induced psoriasis, H&E staining was carried out on the mouse back skin on day 7 of treatment. Skin samples were fixed and stained with H&E, as shown in Fig. 5B and C. The histological evaluation of the mice treated with topical IMQ revealed extensive psoriasis-like lesions, as demonstrated by hyperkeratosis, the skin barrier destruction, and modest dermal inflammation in the epidermal cuticles of the mice. However, these changes were dramatically attenuated in the groups treated with CPT, **5i**, and **5l** (Fig. 5C). These results suggest that **5i** and **5l** may be of potential value for improving psoriasis-like symptoms in the skin.

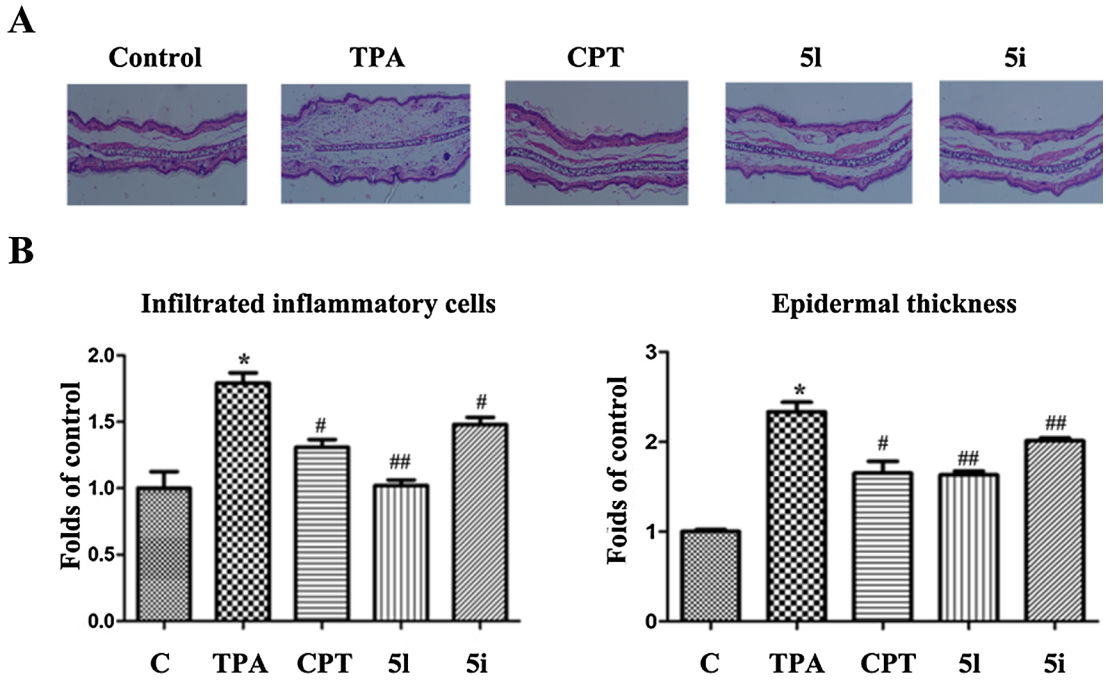

Fig. 3. (A) H&E staining for histological changes of TPA-induced mouse model. (B) Epidermal thickness and infiltrated inflammatory cells folds of control group. C, the control group, TPA, the topical TPA-treated group, CPT, **5i**, and **5l**, 5 μM compounds + TPA are indicated. Values are expressed as the mean ± SD (n = 3). ANOVA followed by Bonferroni's multiple comparison tests was used. (*) $p < 0.05$ and (**) $p < 0.01$ versus control group treated with vehicle, (#) $p < 0.05$ and (##) $p < 0.01$ versus Ac/TPA-treated group.

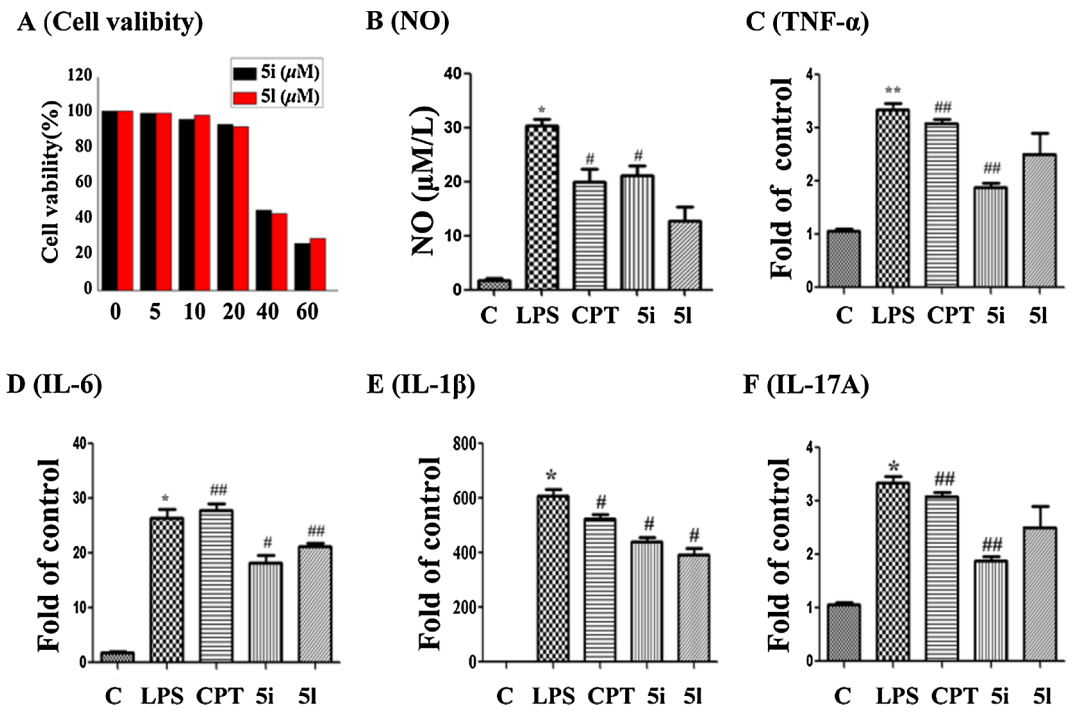

Fig. 4. (A) Determination of the no toxic concentration of **5i** and **5l** against HaCaT cells. (B) **5i** and **5l** inhibited the production of NO in LPS (1 μg/mL)-stimulated HaCaT cells. (C–F) **5i** and **5l** inhibited the mRNA expression levels of inflammatory cytokines in LPS-stimulated HaCaT cells. The mRNA expression level of TNF-α (C), IL-6 (D), IL-1β (E) and IL-17A were inhibited by **5i** and **5l**. C, the control group, LPS, the topical LPS-treated group, CPT, 1 μM + TPA, **5i** and **5l**, 10 μM + TPA are indicated. Values are expressed as the mean ± SD (n = 3). ANOVA followed by Bonferroni's multiple comparison tests was used. (*) $p < 0.05$ and (**) $p < 0.01$ versus control group, (#) $p < 0.05$ and (##) $p < 0.01$ versus LPS group.

2.6. Compounds 5i and 5l suppress the expression of the key cytokines implicated in psoriasis

Since compounds **5i** and **5l** showed potential antipsoriasis activity in vivo, the underlying mechanism of action of **5i** and **5l** was further investigated. First, direct effects of **5i** and **5l** on IMQ-induced cytokines were evaluated using immunohistochemistry staining. It has been reported that the development of the IMQ-induced psoriasis-like skin in mice is mediated via the IL-23/IL-17 axis [29]. IL-23, secreted by dendritic cells, can induce the proliferation of T helper 17 (Th17) cells, which can, in turn, activate and secrete IL-17A, IL-22, and IL-23 [45]. Our results indicated that the expression levels of these key cytokines was significantly higher in the topical IMQ-treated group than that in the control group (Fig. 6A–C). However, the expression levels of these cytokines were significantly lower in the CPT-, **5i-**, and **5l**-treated groups than those in the topical IMQ-treated group. In addition, IMQ application increased the transcription of TNF-α and IFN-γ, two key proinflammatory cytokines involved in the Th17 response [46], while, CPT, **5i**, and **5l** treatment dramatically reduced the expression of TNF-α and IFN-γ (Fig. 6D and E). Thus, oral administration of **5i** and **5l** suppressed the expression of inflammatory cytokines implicated in psoriasis, including IL-17A, IL-22, IL-23, TNF-α, and IFN-γ.

To further examine the effects of **5i** and **5l** on the expression of cytokines associated with psoriasis, quantitative reverse transcription–polymerase chain reaction (RT–PCR) analysis was used to study the mRNA expression of key cytokines and inflammatory mediator in skin lesions after IMQ treatment. The results presented in Fig. 7 demonstrated a marked increase in the mRNA expression of IL-17A, IL-22, IL-23, TNF-α, p65, and IFN-γ in the IMQ-treated group. However, **5i**, **5l**, and CPT pretreatment significantly downregulated the mRNA expression of the genes encoding these inflammatory factors implicated in psoriasis.

To better assign the mechanism of action of **5i** and **5l** on antipsoriasis, these two compounds were examined for their effects on the expression levels of these psoriasis-related markers using western blot analysis. As presented in Fig. 8, topical application of IMQ upregulated the expression levels of all these tested proteins. Whereas, a pretreatment with CPT, **5i**, and **5l** significantly downregulated the expression levels of IL-17A, IL-22 and IL-23, as well as p65, TNF-α, and IFN-γ, but in less extent. These findings are consistent with the results obtained by immunohistochemistry staining and the RT–PCR assay. All these results demonstrated that **5i** and **5l** displayed potential antipsoriasis activity by suppressing the expression of key cytokines and inflammatory mediators such as p65, IL-17, IL-22, IL-23, TNF-α, and IFN-γ.

3. Conclusion

Psoriasis is a skin disorder with a complicated pathophysiology, which has not been fully elucidated yet. Although certain agents have shown clinical success, the treatment of psoriasis remains a significant problem. [55] In this study, we presented a novel strategy to treat psoriasis with small molecules inhibiting the Topo I activity. A series of QCs were synthesized and identified as potent Topo I inhibitors. Some QCs showed potential anti-inflammatory activity against TPA-induced mouse ear inflammation. The most potent Topo I inhibitors and anti-inflammatory agents, **5i** and **5l**, exhibited moderate cytotoxicity against HaCaT cells. These two compounds significantly suppressed the production of NO and the expression levels of inflammatory cytokines such as IL-17, IL-1β, IL-6, and TNF-α in LPS-stimulated HaCaT cells. Moreover, we found that oral gavage of **5i** and **5l** (50 mg/kg), followed by IMQ application to the dorsal skin once daily for seven consecutive days, significantly ameliorated psoriasis symptoms, including an erythema, scaling, and epidermal thickness, compared with those in the vehicle-treated IMQ-induced model mice. These two compounds were then studied for their action against psoriasis in vivo. The results revealed that **5i** and **5l** dramatically inhibited the mRNA expression levels of cytokines and inflammatory mediators, including IL-17A, IL-22, IL-23, p65, TNF-α, and IFN-γ, implicated in psoriasis induced by IMQ in

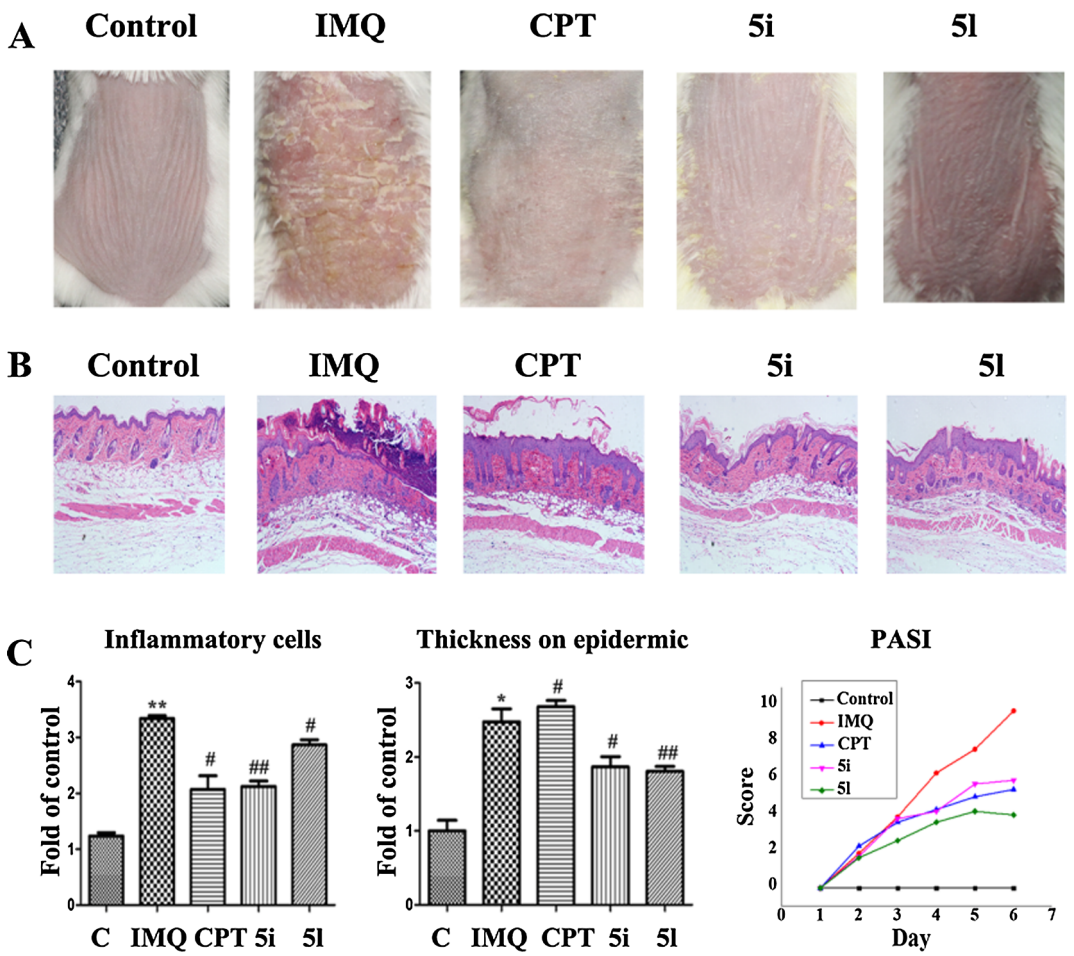

Fig. 5. (A) Images of psoriatic skin lesions treatment with **5i** and **5l**. Photos were taken after 7 days of treatment. (B) Histopathological view of psoriatic skin lesions on treatment with CPT, **5i**, and **5l**. H&E-stained paraffin sections, 200×. (C) Data on epidermal thickness, inflammatory cell and PASI scales in psoriatic skin lesions. C, the control group, IMQ, the topical IMQ-treated group, CPT, 5 mg/kg + IMQ, **5i** and **5l**, 50 mg/kg + IMQ are indicated. Values are expressed as the mean ± SD (n = 6). ANOVA followed by Bonferroni's multiple comparison tests was used. (*) $p < 0.05$ and (**) $p < 0.01$ versus control group, (#) $p < 0.05$ and (##) $p < 0.01$ versus IMQ group.

the back skin of BALB/c mice. Collectively, compounds **5i** and **5l** obtained here could be potential candidates for the treatment of psoriasis. Therefore, the study provided evidence to support the hypothesis that chemical inhibition of Topo I is likely to be an effective strategy for the treatment of psoriasis.

4. Experiment section

4.1. Chemistry

All of the reagents were commercially available and purchased from Sigma-Aldrich Chemical Co., TCI Chemicals, AlfaAesar, and Aladdin (China), which used without further purification. HPLC grade methanol was order from Sinopharm (China) and silica gel (200–300 mesh, Qingdao Haiyang Chemical Co., Ltd). ^{1}H and ^{13}C NMR spectra were recorded using TMS as the internal standard in DMSO-d_6 with a Bruker BioSpin GmbH spectrometer at 400 MHz and 101 MHz, respectively. The chemical shifts are reported in parts per million (ppm) relative to residual DMSO-d_6 ($\delta = 2.50$, ^{1}H, $\delta = 39.5$, ^{13}C) in the deuterium agent. The following abbreviations are used to designate multiplicities: s, single, d, double, t, triplet, q, quartet, m, multiplet, dd, double-double, br s, broad signal. Melting point (mp) was determined using an SRS-OptiMelt automated melting point instrument. High-resolution mass spectra (HR ESI-MS) were recorded on Shimadzu LCMS-IT-TO. The purities of QCs were confirmed by analytical HPLC performed with a dual pump Shimadzu LC-20AB system equipped with an Ultimate XB-C18 column and eluted with methanol/water (80%) at a flow rate of 0.8 mL·min^{-1}.

4.2. General procedure for the synthesis of intermediates 2a-g

To the solution of **1a-g** (1.55 mmol) and ethyl acetoacetate (2.02 g, 1.55 mmol) was added PPA (12.5 g). The reaction mixture was stirred at 130 °C for 2 h. Reaction completion was monitored by TLC. The reaction mixture was poured into ice water slowly with vigorous stirring and the pH was then adjusted to 7–8 using NaOH. The precipitated solid was filtered and dried in vacuum oven get the products. The products were taken for the next reaction without further purification.

4.3. General procedure for the synthesis of intermediates 3a-v

The solution of **2a–g** (10 mmol) in DMF (20 mL) was added the appropriate benzyl bromide (30 mmol) and K_2CO_3 (50 mmol), and the reaction mixture was stirred at room temperature for 8 h. It was then diluted with DCM (80 mL) and H_2O (80 mL). The organic layer was separated, and the aqueous layer was extracted with DCM (80 mL × 2). The combined organic layers were dried over Mg_2SO_4 and concentrated *in vacuo* to provide a crude product, which was purified by column chromatography to yield the title compounds **3a-v**, respectively.

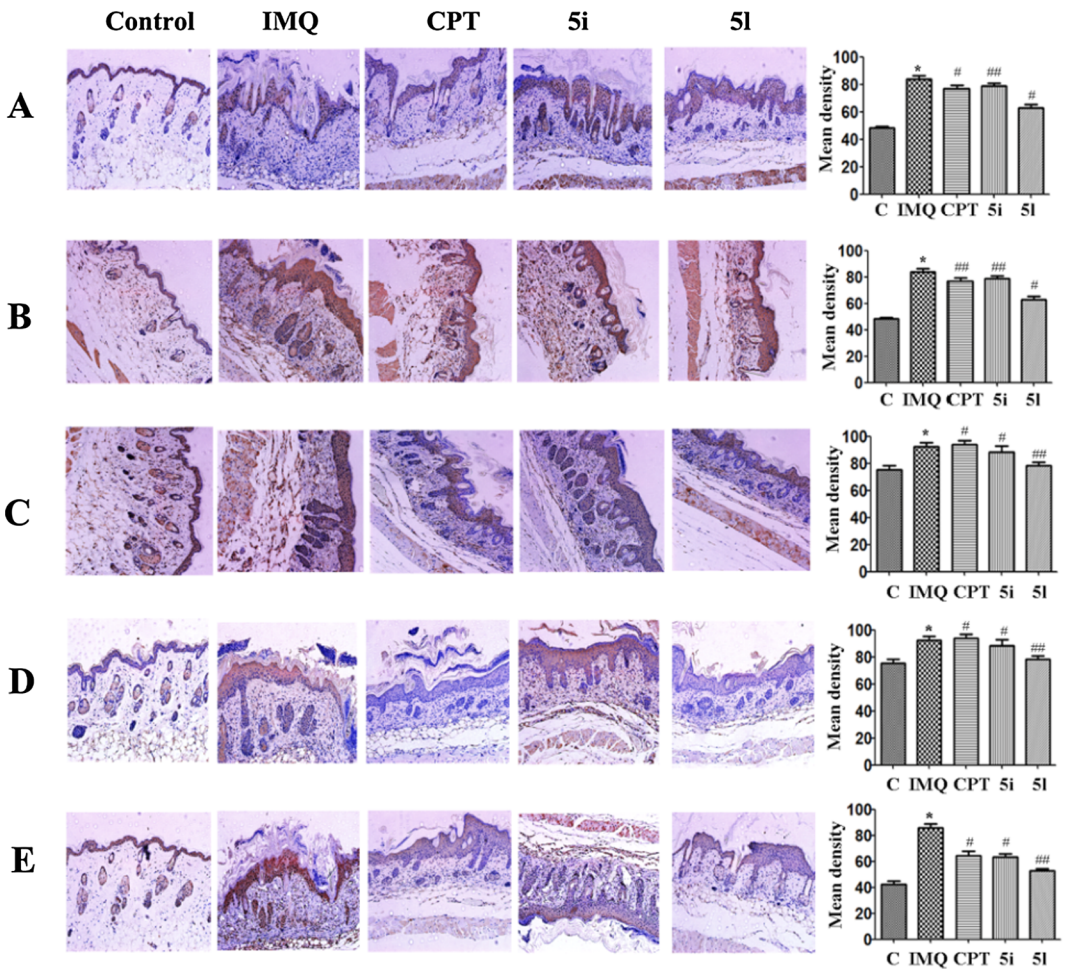

Fig. 6. BALB/c mice were treated as indicated in Experiment Section. After treatment of 7 days, mice were sacrificed, and the back skin section were strained by immunohistochemistry to detect related cytokines in control, IMQ, CPT, **5i**, and **5l**-treated group. (A) IL-17A. (B) IL-22. (C) IL-23. (D) TNF-α. (E) IFN-γ. C, the control group, IMQ, the topical IMQ-treated group, CPT, 5 mg/kg + IMQ, **5i** and **5l**, 50 mg/kg + IMQ are indicated. Values are expressed as the mean ± SD (n = 6). ANOVA followed by Bonferroni's multiple comparison tests was used. (*) $p < 0.05$ and (**) $p < 0.01$ versus control group treated with vehicle, (#) $p < 0.05$ and (##) $p < 0.01$ versus IMQ group.

4.4. General procedure for the synthesis of intermediates 4a-v

Compounds **3a-v** (5 mmol) was dissolved in 20 mL of dioxane and then added to 30 mL of dioxane suspension with SeO_2 (7.5 mmol). The mixture was reacted at 80 °C for 1.5 h under N_2 atmosphere, and 100 mL of ethyl acetate was added for dilution followed by washing once with water. Solvents were removed *in vacuo*, and purification by column chromatography to yield the title compounds **4a-v**, respectively.

4.5. General procedure for the synthesis of 5a-5y

A mixture of the appropriate aldehydes (**4a-v,** 1.0 mmol), the rhodanine moiety (1.1 mmol), and NaOAc (3.0 mmol) in acetic acid (10 mL) heated to 110 °C for 4 h. Then, it was cooled to room temperature and poured into water (50 mL). The product was then filtered through the suction pump, washed with water/EtOH (1/1, v/v) to remove the excess acetic acid and recrystallized from EtOH.

4.5.1. (E)-2-(5-((4-(benzyloxy)quinolin-2-yl)methylene)-4-oxo-2-thioxothiazolidin- 3-yl) acetic acid (5a)

Rhodanine-3-acetic acid and **4a** were used as reactants to give **5a**. Yellow solid, yield: 81%, mp: 231.4–232.6 °C. ^{1}H NMR (400 MHz, DMSO-d_6) δ 8.16 (d, J = 8.2 Hz, 1H), 8.08 (d, J = 8.4 Hz, 1H), 7.92 (s, 1H), 7.82 (t, J = 7.2, 1H), 7.74 (s, 1H), 7.66–7.58 (m, 3H), 7.49–7.43 (m, 2H), 7.40 (t, J = 7.2 Hz, 1H), 5.43 (s, 2H), 4.74 (s, 2H). ^{13}C NMR (101 MHz, DMSO-d_6) δ 200.7, 167.8, 166.9, 162.0, 153.1, 148.5, 136.2, 131.5, 129.7, 129.3, 129.0, 128.8, 128.6, 128.4, 127.8, 122.2, 120.4, 106.0, 70.7, 45.2. HR ESI-MS $(M + H)^+$ m/z = 437.0626 (Cacld for $C_{22}H_{16}N_2O_4S_2$) 437.0621, HPLC purity: 95.4%.

4.5.2. (E)-2-(5-((4-((3,5-dimethylbenzyl)oxy)quinolin-2-yl)methylene)-4-oxo-2- thioxothiazolidin-3-yl)acetic acid (5b)

Rhodanine-3-acetic acid and **4b** were used as reactants to give **5b**. Yellow solid, yield: 76%, mp: 245.3–246.8 °C. ^{1}H NMR (400 MHz, DMSO-d_6) δ 13.41 (br s, 1H), 8.19 (d, J = 8.2 Hz, 1H), 8.11 (d, J = 8.5 Hz, 1H), 7.95 (s, 1H), 7.87–7.82 (m, 1H), 7.74 (s, 1H), 7.66 (t, J = 7.5 Hz, 1H), 6.77–6.71 (m, 2H), 6.52 (t, J = 2.1 Hz, 1H), 5.36 (s, 2H), 4.77 (s, 2H), 3.77 (s, 6H). ^{13}C NMR (101 MHz, DMSO-d_6) δ 200.7, 167.8, 166.8, 161.9, 161.2, 153.0, 148.4, 138.4, 131.5, 129.7, 128.8, 128.5, 127.8, 122.2, 120.3, 106.3, 105.9, 100.3, 70.6, 55.7, 45.0. HR ESI-MS $(M + H)^+$ m/z = 497.0878 (Cacld for $C_{24}H_{20}N_2O_6S_2$) 497.0881, HPLC purity: 96.3%.

4.5.3. (E)-2-(5-((4-((4-chlorobenzyl)oxy)quinolin-2-yl)methylene)-4-oxo-2- thioxothiazolidin-3-yl)acetic acid (5c)

Rhodanine-3-acetic acid and **4c** were used as reactants to give **5c**. Yellow solid, yield: 79%, mp: 213.6–215.3 °C. ^{1}H NMR (400 MHz, DMSO-d_6) δ 13.40 (br s, 1H), 8.19 (d, J = 8.2 Hz, 1H), 8.12 (d, J = 8.4 Hz, 1H), 7.96 (s, 1H), 7.85 (t, J = 7.5 Hz, 1H), 7.76 (s, 1H),

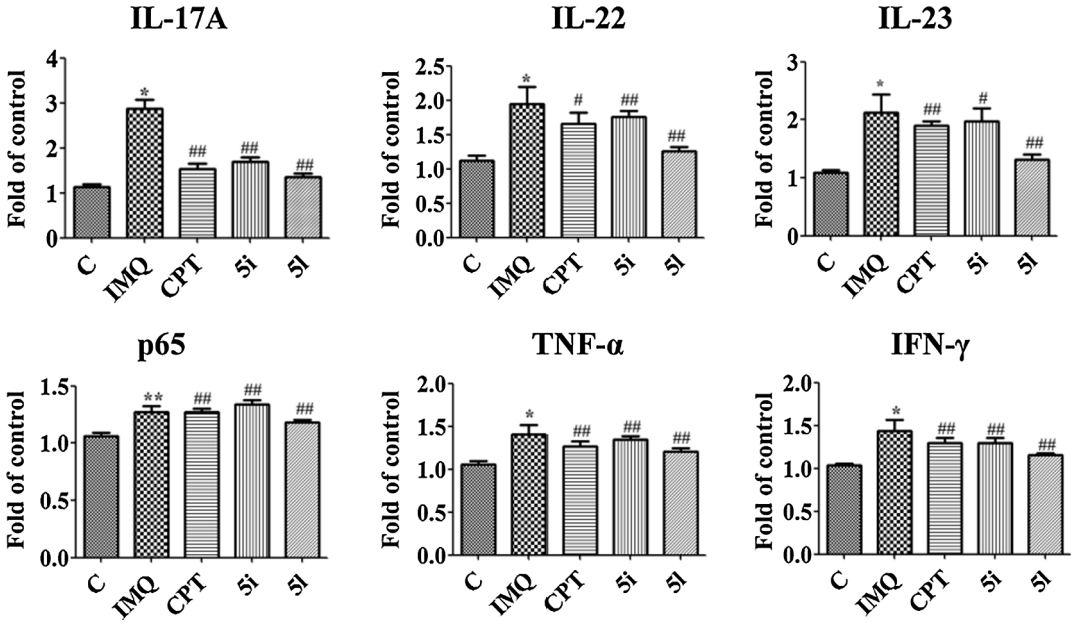

Fig. 7. 5i and **5l** reduces the expression levels of cytokines associated with psoriasis. The expression levels of IL-17A, IL-22, IL-23, TNF-α, P65, and IFN-γ were detected by quantitative RT-PCR. C, the control group, IMQ, the topical IMQ-treated group, CPT, 5 mg/kg + IMQ, **5i** and **5l**, 50 mg/kg + IMQ are indicated. Values are expressed as the mean ± SD (n = 6). ANOVA followed by Bonferroni's multiple comparison tests was used. (*) $p < 0.05$ and (**) $p < 0.01$ versus control group treated with vehicle, (#) $p < 0.05$ and (##) $p < 0.01$ versus IMQ group.

7.69–7.63 (m, 3H), 7.57 (d, J = 8.2 Hz, 2H), 5.43 (s, 2H), 4.77 (s, 2H). ^{13}C NMR (101 MHz, DMSO-d_6) δ 200.7, 167.8, 166.9, 161.8, 153.1, 148.5, 135.7, 132.1, 131.6, 130.6, 129.7, 128.8, 128.6, 127.9, 122.2, 122.0, 120.3, 106.0, 69.9, 45.1. HR ESI-MS (M + H)$^+$ m/z = 471.0232 (Cacld for $C_{22}H_{15}ClN_2O_4S_2$) 471.0226, HPLC purity: 97.2%.

4.5.4. (E)-2-(5-((4-((4-bromobenzyl)oxy)quinolin-2-yl)methylene)-4-oxo-2- thioxothiazolidin-3-yl)acetic acid (5d)

Rhodanine-3-acetic acid and **4d** were used as reactants to give **5d**. Yellow solid, yield: 82%, mp: 239.6–241.4 °C. ^{1}H NMR (400 MHz, DMSO-d_6) δ 13.40 (s, 1H), 8.19 (d, J = 8.1 Hz, 1H), 8.12 (d, J = 8.5 Hz, 1H), 7.97 (s, 1H), 7.85 (t, J = 7.4 Hz, 1H), 7.77 (s, 1H), 7.69–7.61 (m, 3H), 7.52 (d, J = 8.3 Hz, 2H), 5.45 (s, 2H), 4.77 (s, 2H). ^{13}C NMR (101 MHz, DMSO-d_6) δ 200.7, 167.8, 166.9, 161.9, 153.1, 148.5, 135.3, 133.5, 131.6, 130.3, 129.7, 129.1, 128.8, 128.6, 127.9, 122.2, 120.3, 106.1, 69.9, 45.1. HR ESI-MS (M + H)$^+$ m/z = 514.9778 (Cacld for $C_{22}H_{15}BrN_2O_4S_2$) 514.9786, HPLC purity: 96.6%.

4.5.5. (E)-2-(5-((4-((4-nitrobenzyl)oxy)quinolin-2-yl)methylene)-4-oxo-2- thioxothiazolidin-3-yl)acetic acid (5e)

Rhodanine-3-acetic acid and **4e** were used as reactants to give **5e**. Yellow solid, yield: 85%, mp: 222.9–224.3 °C. ^{1}H NMR (400 MHz, DMSO-d_6) δ 13.39 (br s, 1H), 8.31 (d, J = 8.6 Hz, 2H), 8.25 (d, J = 8.2 Hz, 1H), 8.13 (d, J = 8.4 Hz, 1H), 7.94 (s, 1H), 7.91–7.83 (m, 3H), 7.75 (s, 1H), 7.68 (t, J = 7.6 Hz, 1H), 5.62 (s, 2H), 4.77 (s, 2H). ^{13}C NMR (101 MHz, DMSO-d_6) δ 200.7, 167.8, 166.8, 161.6, 153.0, 148.5, 147.8, 143.9, 131.6, 129.6, 129.0, 128.8, 128.6, 127.9, 124.2, 122.2, 120.2, 106.0, 69.4, 45.0. HR ESI-MS (M + H)$^+$ m/z = 482.0413 (Cacld for $C_{22}H_{15}N_3O_6S_2$) 482.0419, HPLC purity: 98.2%.

4.5.6. (E)-2-(5-((4-((4-methylbenzyl)oxy)quinolin-2-yl)methylene)-4-oxo-2- thioxothiazolidin-3-yl)acetic acid (5f)

Rhodanine-3-acetic acid and **4f** were used as reactants to give **5f**. Yellow solid, yield: 73%, mp: 198.7–200.4 °C. ^{1}H NMR (400 MHz, DMSO-d_6) δ 8.12 (d, J = 8.2 Hz, 1H), 8.05 (d, J = 8.4 Hz, 1H), 7.89 (s,

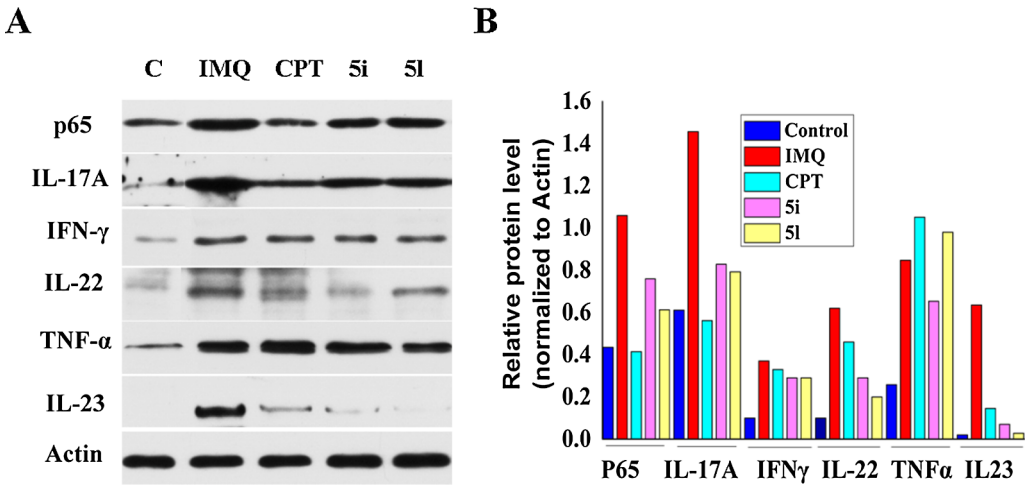

Fig. 8. 5i and **5l** suppress the expression of cytokines associated with psoriasis. C, the control group, IMQ, the topical IMQ-treated group, CPT, 5 mg/kg + IMQ, **5l** and **5i**, 50 mg/kg + IMQ are indicated.

1H), 7.80 (t, J = 7.5 Hz, 1H), 7.68 (s, 1H), 7.60 (t, J = 7.5 Hz, 1H), 7.48 (d, J = 7.8 Hz, 2H), 7.26 (d, J = 7.8 Hz, 2H), 5.35 (s, 2H), 4.75 (s, 2H), 2.33 (s, 3H). ^{13}C NMR (101 MHz, DMSO-d_6) δ 200.8, 167.8, 166.8, 162.0, 153.0, 148.4, 138.2, 133.2, 131.4, 129.8, 129.6, 128.7, 128.5, 128.3, 127.7, 122.2, 120.4, 105.9, 70.7, 45.0, 21.3. HR ESI-MS $(M + H)^+$ m/z = 451.0762 (Cacld for $C_{23}H_{18}N_2O_4S_2$) 451.0758, HPLC purity: 96.4%.

4.5.7. (E)-2-(5-((4-((4-cyanobenzyl)oxy)quinolin-2-yl)methylene)-4-oxo-2-thioxothiazolidin-3-yl)acetic acid (5g)

Rhodanine-3-acetic acid and **4g** were used as reactants to give **5g**. Yellow solid, yield: 88%, mp: 217.6–218.9 °C. ^{1}H NMR (400 MHz, DMSO-d_6) δ 8.20 (d, J = 8.2 Hz, 1H), 8.07 (d, J = 8.4 Hz, 1H), 7.93 (d, J = 8.2 Hz, 2H), 7.87 (s, 1H), 7.83 (t, J = 8.2 Hz, 1H), 7.78 (d, J = 8.2 Hz, 2H), 7.68 (s, 1H), 7.67–7.61 (m, 1H), 5.52 (s, 2H), 4.76 (s, 2H). ^{13}C NMR (101 MHz, DMSO-d_6) δ 200.7, 167.8, 166.8, 161.6, 153.0, 148.4, 141.9, 133.0, 131.6, 129.6, 128.8, 128.7, 128.6, 127.9, 122.2, 120.2, 119.1, 111.4, 105.9, 69.6, 45.0. HR ESI-MS $(M + H)^+$ m/z = 462.0554 (Cacld for $C_{23}H_{15}N_3O_4S_2$) 462.0559, HPLC purity: 97.8%.

4.5.8. (E)-2-(4-oxo-2-thioxo-5-((4-((4-(trifluoromethyl)benzyl)oxy) quinolin-2-yl) methylene)thiazolidin-3-yl)acetic acid (5 h)

Rhodanine-3-acetic acid and **4h** were used as reactants to give **5h**. Yellow solid, yield: 86%, mp: 231.8–233.9 °C. ^{1}H NMR (400 MHz, DMSO-d_6) δ 8.13 (d, J = 8.2 Hz, 1H), 7.98 (d, J = 8.4 Hz, 1H), 7.83–7.75 (m, 6H), 7.62–7.56 (m, 2H), 5.46 (s, 2H), 4.72 (s, 2H). ^{13}C NMR (101 MHz, DMSO-d_6) δ 200.7, 167.8, 166.8, 161.6, 152.8, 148.3, 141.0, 131.4, 129.5, 129.2, 128.7, 128.6, 128.4, 127.7, 125.9 (q, J = 274.5 Hz), 124.6, 122.1, 120.1, 105.8, 69.6, 45.0. HR ESI-MS $(M + H)^+$ m/z = 505.0437 (Cacld for $C_{23}H_{15}F_3N_3O_4S_2$) 505.0442, HPLC purity: 98.4%.

4.5.9. (E)-2-(5-((4-((4-bromo-2-fluorobenzyl)oxy)quinolin-2-yl) methylene)-4-oxo-2-thioxothiazolidin-3-yl)acetic acid (5i)

Rhodanine-3-acetic acid and **4i** were used as reactants to give **5i**. Yellow solid, yield: 82%, mp: 246.4–248.1 °C. ^{1}H NMR (400 MHz, DMSO-d_6) δ 8.11 (d, J = 8.5 Hz, 1H), 8.08 (d, J = 8.6 Hz, 1H), 7.93 (s, 1H), 7.85–7.80 (m, 1H), 7.77 (s, 1H), 7.72–7.65 (m, 2H), 7.62 (t, J = 7.6 Hz, 1H), 7.54–7.50 (m, 1H), 5.44 (s, 2H), 4.76 (s, 2H). ^{13}C NMR (101 MHz, DMSO-d_6) δ 200.7, 167.9, 166.8, 161.6, 160.7, 153.0, 148.4, 132.4 (d, J = 4.4 Hz), 131.6, 129.7, 128.8, 128.6, 128.4 (d, J = 3.5 Hz), 127.9, 122.8 (d, J = 14.5 Hz), 122.7 (d, J = 9.7 Hz), 122.1, 120.1, 119.5, 105.9, 64.6, 45.0. HR ESI-MS $(M + H)^+$ m/z = 532.9652 (Cacld for $C_{22}H_{14}BrFN_2O_4S_2$) 532.9661, HPLC purity: 97.3%.

4.5.10. (E)-2-(5-((4-((3,5-difluorobenzyl)oxy)quinolin-2-yl)methylene)-4-oxo-2- thioxothiazolidin-3-yl)acetic acid (5j)

Rhodanine-3-acetic acid and **4j** were used as reactants to give **5j**. Yellow solid, yield: 71%, mp: 266.8–268.5 °C. ^{1}H NMR (400 MHz, DMSO-d_6) δ 8.11–8.03 (m, 2H), 7.91 (s, 1H), 7.83–7.77 (m, 2H), 7.73 (s, 1H), 7.59 (t, J = 7.6 Hz, 1H), 7.40–7.34 (m, 1H), 7.22–7.16 (m, 1H), 5.42 (s, 2H), 4.75 (s, 2H). ^{13}C NMR (101 MHz, DMSO-d_6) δ 200.7, 167.9, 166.8, 163.6, 161.6, 153.0, 148.4, 132.6 (d, J = 10.1 Hz), 131.5, 129.7, 128.7, 128.5, 127.8, 122.7, 122.1, 120.1, 119.7 (d, J = 3.6 Hz), 112.3 (d, J = 3.8 Hz), 105.9, 104.7 (d, J = 25.7 Hz), 64.7, 45.0. HR ESI-MS $(M + H)^+$ m/z = 473.0419 (Cacld for $C_{22}H_{14}F_2N_2O_4S_2$) 473.0425, HPLC purity: 98.1%.

4.5.11. (E)-2-(5-((4-((3,4-difluorobenzyl)oxy)quinolin-2-yl)methylene)-4-oxo-2- thioxothiazolidin-3-yl)acetic acid (5k)

Rhodanine-3-acetic acid and **4k** were used as reactants to give **5k**. Yellow solid, yield: 75%, mp: 263.7–265.2 °C. ^{1}H NMR (400 MHz, DMSO-d_6) δ 8.13 (d, J = 8.2 Hz, 1H), 8.02 (d, J = 8.4 Hz, 1H), 7.84 (s, 1H), 7.79 (t, J = 7.5 Hz, 1H), 7.70–7.58 (m, 3H), 7.54–7.43 (m, 2H), 5.36 (s, 2H), 4.74 (s, 2H). ^{13}C NMR (101 MHz, DMSO-d_6) δ 200.7, 167.8, 166.8, 161.6, 152.9, 151.3, 149.9 (d, J = 12.5 Hz), 148.4, 133.9 (d, J = 5.9 Hz), 131.5, 129.6, 128.7, 128.5, 127.8, 125.4 (d, J = 6.7 Hz), 122.2, 120.2, 118.2 (d, J = 17.2 Hz), 117.6 (d, J = 17.5 Hz), 105.8, 69.3, 45.0. HR ESI-MS $(M + H)^+$ m/z = 473.0417 (Cacld for $C_{22}H_{14}F_2N_2O_4S_2$) 473.0425, HPLC purity: 95.3%.

4.5.12. (E)-2-(5-((4-((4-fluorobenzyl)oxy)quinolin-2-yl)methylene)-4-oxo-2- thioxothiazolidin-3-yl)acetic acid (5l)

Rhodanine-3-acetic acid and **4l** were used as reactants to give **5l**. Yellow solid, yield: 86%, mp: 231.8–233.9 °C. ^{1}H NMR (400 MHz, DMSO-d_6) δ 13.40 (br s, 1H), 8.17 (d, J = 8.3 Hz, 1H), 8.12 (d, J = 8.5 Hz, 1H), 7.98 (s, 1H), 7.85 (t, J = 7.6 Hz, 1H), 7.79 (s, 1H), 7.69–7.61 (m, 3H), 7.29 (t, J = 8.8 Hz, 2H), 5.43 (s, 2H), 4.77 (s, 2H). ^{13}C NMR (101 MHz, DMSO-d_6) δ 200.7, 167.8, 166.8, 162.6, 161.8, 153.0, 148.4, 132.5 (d, J = 3.0 Hz), 131.5, 130.8 (d, J = 8.4 Hz), 129.7, 128.7, 128.5, 127.8, 122.2, 120.3, 116.0 (d, J = 21.5 Hz), 105.9, 70.0, 45.0. HR ESI-MS $(M + H)^+$ m/z = 455.0526 (Cacld for $C_{22}H_{15}FN_2O_4S_2$) 455.0532, HPLC purity: 97.5%.

4.5.13. (E)-2-(5-((4-((3-fluorobenzyl)oxy)quinolin-2-yl)methylene)-4-oxo-2- thioxothiazolidin-3-yl)acetic acid (5m)

Rhodanine-3-acetic acid and **4m** were used as reactants to give **5m**. Yellow solid, yield: 86%, mp: 231.8–233.9 °C. ^{1}H NMR (400 MHz, DMSO-d_6) δ 8.14 (d, J = 8.2 Hz, 1H), 8.02 (d, J = 8.4 Hz, 1H), 7.83 (s, 1H), 7.79 (t, J = 7.6 Hz, 1H), 7.65–7.58 (m, 2H), 7.53–7.47 (m, 1H), 7.45–7.41 (m, 2H), 7.27–7.19 (m, 1H), 5.40 (s, 2H), 4.73 (s, 2H). ^{13}C NMR (101 MHz, DMSO-d_6) δ 200.7, 167.8, 166.8, 162.7, 161.7, 152.9, 148.4, 139.0 (d, J = 7.6 Hz), 131.5, 131.2 (d, J = 8.3 Hz), 129.6, 128.7, 128.4, 127.8, 124.2 (d, J = 2.7 Hz), 122.2, 120.2, 115.6 (d, J = 20.9 Hz), 115.0 (d, J = 22.0 Hz), 105.8, 69.8, 45.0. HR ESI-MS $(M + H)^+$ m/z = 455.0537 (Cacld for $C_{22}H_{15}FN_2O_4S_2$) 455.0532, HPLC purity: 96.9%.

4.5.14. (E)-2-(5-((4-((2-fluorobenzyl)oxy)quinolin-2-yl)methylene)-4-oxo-2- thioxothiazolidin-3-yl)acetic acid (5n)

Rhodanine-3-acetic acid and **4n** were used as reactants to give **5n**. Yellow solid, yield: 86%, mp: 231.8–233.9 °C. ^{1}H NMR (400 MHz, DMSO-d_6) δ 13.45 (br s, 1H), 8.09 (d, J = 8.3 Hz, 1H), 8.05 (d, J = 8.4 Hz, 1H), 7.90 (s, 1H), 7.82–7.78 (m, 1H), 7.77–7.71 (m, 2H), 7.63–7.57 (m, 1H), 7.52–7.46 (m, 1H), 7.35–7.28 (m, 2H), 5.45 (s, 2H), 4.74 (s, 2H). ^{13}C NMR (101 MHz, DMSO-d_6) δ 200.7, 167.9, 166.8, 161.7, 160.9, 153.0, 148.4, 131.5, 131.3 (d, J = 8.3 Hz), 131.0 (d, J = 3.8 Hz), 129.7, 128.7, 128.5, 127.8, 125.2 (d, J = 3.5 Hz), 123.2 (d, J = 14.3 Hz), 122.1, 120.2, 116.0 (d, J = 20.7 Hz), 105.8, 65.1, 45.0. HR ESI-MS $(M + H)^+$ m/z = 455.4928 (Cacld for $C_{22}H_{15}FN_2O_4S_2$) 455.0532, HPLC purity: 96.2%.

4.5.15. (Z)-2-(5-((6-fluoro-4-((4-fluorobenzyl)oxy)quinolin-2-yl) methylene)-4- oxo-2-thioxothiazolidin-3-yl)acetic acid (5o)

Rhodanine-3-acetic acid and **4o** were used as reactants to give **5o**. Yellow solid, yield: 71%, mp: 262.5–263.9 °C. ^{1}H NMR (400 MHz, DMSO-d_6) δ 13.46 (s, 1H), 8.23– 7.15 (m, 1H), 7.96 (s, 1H), 7.82–7.72 (m, 3H), 7.69–7.65 (m, 2H), 7.31–7.25 (m, 2H), 5.42 (s, 2H), 4.77 (s, 2H). ^{13}C NMR (101 MHz, DMSO-d_6) δ 200.5, 167.8, 166.8, 163.8, 162.6, 161.3, 159.6, 152.6, 145.6, 132.3 (d, J = 3.0 Hz), 131.9 (d, J = 9.2 Hz), 130.8 (d, J = 8.4 Hz), 129.5, 128.5, 121.5 (d, J = 25.9 Hz), 121.1 (d, J = 9.7 Hz), 106.4, 106.1 (d, J = 23.6 Hz), 70.1, 45.0. HR ESI-MS $(M + H)^+$ m/z = 473.0419 (Cacld for $C_{22}H_{14}F_2N_2O_4S_2$) 473.0425, HPLC purity: 97.1%.

4.5.16. (Z)-2-(5-((6-chloro-4-((4-fluorobenzyl)oxy)quinolin-2-yl) methylene)-4- oxo-2-thioxothiazolidin-3-yl)acetic acid (5p)

Rhodanine-3-acetic acid and **4p** were used as reactants to give **5p**. Yellow solid, yield: 78%, mp: 253.1–254.6 °C. ^{1}H NMR (400 MHz, DMSO-d_6) δ 13.44 (br s, 1H), 8.08 (d, J = 9.0 Hz, 1H), 8.05 (d,

J = 2.3 Hz, 1H), 7.92 (s, 1H), 7.86–7.75 (m, 2H), 7.70–7.64 (m, 2H), 7.33–7.25 (m, 2H), 5.40 (s, 2H), 4.77 (s, 2H). ^{13}C NMR (101 MHz, DMSO-d_6) δ 200.4, 167.8, 166.8, 162.6, 160.9, 153.4, 146.7, 132.3, 132.2 (d, J = 3.0 Hz), 131.9, 130.9 (d, J = 8.4 Hz), 130.8, 129.3, 128.9, 121.0, 120.9, 116.0 (d, J = 21.5 Hz), 106.6, 70.2, 45.0. HR ESI-MS $(M + H)^+$ m/z = 489.0138 (Cacld for $C_{22}H_{14}ClFN_2O_4S_2$) 489.0142, HPLC purity: 97.1%.

4.5.17. (Z)-2-(5-((4-((4-fluorobenzyl)oxy)-6-methylquinolin-2-yl) methylene)-4- oxo-2-thioxothiazolidin-3-yl)acetic acid (5q)

Rhodanine-3-acetic acid and **4q** were used as reactants to give **5q**. Yellow solid, yield: 88%, mp: 236.7–238.2 °C. ^{1}H NMR (400 MHz, DMSO-d_6) δ 13.44 (br s, 1H), 8.00 (d, J = 8.6 Hz, 1H), 7.93 (s, 1H), 7.91 (s, 1H), 7.72 (s, 1H), 7.71–7.61 (m, 3H), 7.35–7.23 (m, 2H), 5.40 (s, 2H), 4.77 (s, 2H), 2.51 (s, 3H). ^{13}C NMR (101 MHz, DMSO-d_6) δ 200.8, 167.9, 166.8, 162.6, 161.2, 152.0, 147.0, 137.8, 133.6, 132.5 (d, J = 3.1 Hz), 130.9 (d, J = 8.4 Hz), 129.9, 128.6, 127.9, 120.8, 120.2, 116.0 (d, J = 21.5 Hz), 105.9, 69.9, 45.0, 21.9. HR ESI-MS $(M + H)^+$ m/z = 469.0671 (Cacld for $C_{23}H_{17}FN_2O_4S_2$) 469.0668, HPLC purity: 95.5%.

4.5.18. (Z)-2-(5-((4-((4-fluorobenzyl)oxy)-6-nitroquinolin-2-yl) methylene)-4- oxo-2-thioxothiazolidin-3-yl)acetic acid (5r)

Rhodanine-3-acetic acid and **4r** were used as reactants to give **5r**. Yellow solid, yield: 85%, mp: 271.4–272.7 °C. ^{1}H NMR (400 MHz, DMSO-d_6) δ 13.48 (br s, 1H), 8.83 (d, J = 2.5 Hz, 1H), 8.51–8.41 (m, 1H), 8.23 (d, J = 9.3 Hz, 1H), 7.96 (s, 1H), 7.92 (s, 1H), 7.75–7.65 (m, 2H), 7.35–7.27 (m, 2H), 5.46 (s, 2H), 4.78 (s, 2H). ^{13}C NMR (101 MHz, DMSO-d_6) δ 200.1, 167.8, 166.7, 163.1, 162.7, 156.5, 150.2, 145.2, 131.8 (d, J = 3.0 Hz), 131.2 (d, J = 8.4 Hz), 130.7, 130.5, 128.6, 124.7, 119.2, 119.1 (d, J = 20.9 Hz), 116.1 (d, J = 21.5 Hz), 107.2, 70.7, 45.1. HR ESI-MS $(M + H)^+$ m/z = 500.0329 (Cacld for $C_{22}H_{14}FN_3O_6S_2$) 500.0336, HPLC purity: 96.9%.

4.5.19. (Z)-2-(5-((4-((4-fluorobenzyl)oxy)-6-methoxyquinolin-2-yl) methylene)-4- oxo-2-thioxothiazolidin-3-yl)acetic acid (5s)

Rhodanine-3-acetic acid and **4s** were used as reactants to give **5s**. Yellow solid, yield: 80%, mp: 246.6–248.2 °C. ^{1}H NMR (400 MHz, DMSO-d_6) δ 13.40 (s, 1H), 8.02 (d, J = 9.2 Hz, 1H), 7.92 (s, 1H), 7.72 (s, 1H), 7.69–7.63 (m, 2H), 7.52–7.44 (m, 1H), 7.40 (d, J = 2.7 Hz, 1H), 7.31–7.25 (m, 2H), 5.43 (s, 2H), 4.76 (s, 2H), 3.91 (s, 3H). ^{13}C NMR (101 MHz, DMSO-d_6) δ 200.7, 167.9, 166.9, 162.5, 160.5, 158.7, 150.4, 144.4, 132.6, 132.5, 130.7 (d, J = 8.3 Hz), 130.1, 127.1, 123.6, 121.4, 116.0 (d, J = 21.5 Hz), 106.2, 100.3, 69.8, 56.1, 45.0. HR ESI-MS $(M + H)^+$ m/z = 485.0658 (Cacld for $C_{23}H_{17}FN_2O_5S_2$) 485.0662, HPLC purity: 98.4%.

4.5.20. (Z)-2-(5-((4-((4-fluorobenzyl)oxy)-6-(trifluoromethoxy)quinolin-2-yl) methylene)-4-oxo-2-thioxothiazolidin-3-yl)acetic acid (5t)

Rhodanine-3-acetic acid and **4t** were used as reactants to give **5t**. Yellow solid, yield: 75%, mp: 234.5–235.8 °C. ^{1}H NMR (400 MHz, DMSO-d_6) δ 13.45 (br s, 1H), 8.25 (d, J = 9.2 Hz, 1H), 7.98 (s, 1H), 7.97 (d, J = 1.5 Hz, 1H), 7.87 (s, 1H), 7.87–7.75 (m, 1H), 7.71–7.63 (m, 2H), 7.31–7.27 (m, 2H), 5.44 (s, 2H), 4.77 (s, 2H). ^{13}C NMR (101 MHz, DMSO-d_6) δ 200.3, 167.8, 166.8, 162.0, 161.4, 159.5, 154.0, 147.0, 146.7, 132.5 (d, J = 8.1 Hz), 131.7 (d, J = 8.5 Hz), 129.2, 128.4, 125.3 (q, J = 271.5 Hz), 122.6, 120.4, 119.7 (d, J = 20.8 Hz), 112.9, 106.7, 65.0, 45.1. HR ESI-MS $(M + H)^+$ m/z = 539.0372 (Cacld for $C_{23}H_{17}F_4N_2O_5S_2$) 539.0368, HPLC purity: 96.2%.

4.5.21. (Z)-2-(5-((4-((4-bromo-2-fluorobenzyl)oxy)-6-chloroquinolin-2-yl) methylene)-4-oxo-2-thioxothiazolidin-3-yl)acetic acid (5u)

Rhodanine-3-acetic acid and **4u** were used as reactants to give **5u**. Yellow solid, yield: 77%, mp: 236.7–238.4 °C. ^{1}H NMR (400 MHz, DMSO-d_6) δ 13.44 (s, 1H), 8.12 (d, J = 9.0 Hz, 1H), 8.05 (d, J = 2.3 Hz, 1H), 7.94 (s, 1H), 7.85 (s, 1H), 7.89–7.76 (m, 1H), 7.73–7.67 (m, 2H), 7.58–7.48 (m, 1H), 5.45 (s, 2H), 4.77 (s, 2H). ^{13}C NMR (101 MHz, DMSO-d_6) δ 200.3, 167.8, 166.8, 162.7, 160.3, 153.5, 146.8, 134.0, 132.4 (d, J = 8.3 Hz), 132.2, 132.1, 129.2, 129.0, 128.4 (d, J = 21.4 Hz), 122.8, 122.6, 120.9 (d, J = 5.8 Hz), 119.6, 119.4, 106.7, 64.9, 45.05. HR ESI-MS $(M + H)^+$ m/z = 566.9259 (Cacld for $C_{22}H_{13}BrClFN_2O_4S_2$) 566.9251, HPLC purity: 98.3%.

4.5.22. (Z)-2-(5-((4-((4-bromo-2-fluorobenzyl)oxy)-6-(trifluoromethoxy) quinolin-2-yl)methylene)-4-oxo-2-thioxothiazolidin-3-yl)acetic acid (5v)

Rhodanine-3-acetic acid and **4v** were used as reactants to give **5v**. Yellow solid, yield: 84%, mp: 229.3–230.8 °C. ^{1}H NMR (400 MHz, DMSO-d_6) δ 13.44 (br s, 1H), 8.26 (d, J = 9.2 Hz, 1H), 7.99 (s, 1H), 7.95 (d, J = 1.6 Hz, 1H), 7.91 (s, 1H), 7.85–7.79 (m, 1H), 7.75–7.65 (m, 2H), 7.59–7.47 (m, 1H), 5.49 (s, 2H), 4.78 (s, 2H). ^{13}C NMR (101 MHz, DMSO-d_6) δ 200.3, 167.8, 166.8, 162.0, 161.4, 159.5, 154.0, 146.7, 132.5 (d, J = 8.4 Hz), 131.7, 130.9 (d, J = 8.1 Hz), 129.2, 123.4 (q, J = 274.7 Hz), 121.8, 120.6, 119.8, 119.2, 116.0 (d, J = 21.4 Hz), 112.9, 106.7, 65.0, 45.1. HR ESI-MS $(M + H)^+$ m/z = 616.9446 (Cacld for $C_{22}H_{13}BrF_4N_2O_5S_2$) 616.9438, HPLC purity: 98.4%.

4.5.23. (E)-5-((4-((4-bromo-2-fluorobenzyl)oxy)quinolin-2-yl) methylene)-2- thioxothiazolidin-4-one (5w)

Rhodanine and **4i** were used as reactants to give **5w**. Yellow solid, yield: 87%, mp: 217.2–219.1 °C. ^{1}H NMR (400 MHz, DMSO-d_6) δ 13.72 (s, 1H), 8.11–8.03 (m, 2H), 7.80 (t, J = 7.2 Hz, 1H), 7.75–7.64 (m, 4H), 7.60 (t, J = 7.6 Hz, 1H), 7.52 (d, J = 8.2 Hz, 1H), 5.43 (s, 2H). ^{13}C NMR (101 MHz, DMSO-d_6) δ 203.1, 169.7, 162.0, 161.4, 159.5, 153.2, 148.4, 132.5 (d, J = 4.5 Hz), 132.1, 131.5, 128.7, 128.4 (d, J = 3.5 Hz), 127.7, 127.6, 123.0, 122.8 (d, J = 12.0 Hz), 120.0, 119.5, 105.8, 64.6. HR ESI-MS $(M + H)^+$ m/z = 474.9519 (Cacld for $C_{20}H_{12}BrFN_2O_2S_2$) 474.9524, HPLC purity: 96.6%.

4.5.24. (E)-5-((4-((4-bromo-2-fluorobenzyl)oxy)quinolin-2-yl) methylene)-3- ethyl-2-thioxothiazolidin-4-one (5x)

Rhodanine-3-ethyl and **4i** were used as reactants to give **5x**. Yellow solid, yield: 84%, mp: 238.1–239.9 °C. ^{1}H NMR (400 MHz, DMSO-d_6) δ 8.13–8.07 (m, 2H), 7.87 (s, 1H), 7.83 (t, J = 7.6 Hz, 1H), 7.77 (s, 1H), 7.75–7.65 (m, 2H), 7.62 (t, J = 7.6 Hz, 1H), 7.53 (d, J = 8.4 Hz, 1H), 5.45 (s, 2H), 4.08 (q, J = 6.9 Hz, 2H), 1.21 (t, J = 7.1 Hz, 3H). ^{13}C NMR (101 MHz, DMSO-d_6) δ 167.2, 161.6, 160.0, 153.4, 148.6, 132.5 (d, J = 4.4 Hz), 131.5, 129.4, 129.0, 128.8, 128.4, 127.8, 125.6, 123.0 (d, J = 8.3 Hz), 122.9 (d, J = 8.5 Hz), 120.2, 119.8, 119.5 (d, J = 24.4 Hz), 105.9, 64.8, 39.4, 12.6. HR ESI-MS $(M + H)^+$ m/z = 501.9828 (Cacld for $C_{22}H_{16}BrFN_2O_2S_2$) 501.9834, HPLC purity: 97.8%.

4.5.25. (E)-3-(5-((4-((4-bromo-2-fluorobenzyl)oxy)quinolin-2-yl) methylene)-4- oxo-2-thioxothiazolidin-3-yl)propanoic acid (5y)

Rhodanine-3-propanoic acid and **4i** were used as reactants to give **5y**. Yellow solid, yield: 83%, mp: 256.7–257.9 °C. ^{1}H NMR (400 MHz, DMSO-d_6) δ 12.54 (s, 1H), 8.13–8.05 (m, 2H), 7.87 (s, 1H), 7.82 (t, J = 7.6 Hz, 1H), 7.77 (s, 1H), 7.73–7.67 (m, 2H), 7.62 (t, J = 7.6 Hz, 1H), 7.53 (d, J = 9.6 Hz, 1H), 5.44 (s, 2H), 4.27 (t, J = 8.2 Hz, 2H), 2.65 (t, J = 7.1 Hz, 2H). ^{13}C NMR (101 MHz, DMSO-d_6) δ 200.7, 172.3, 167.2, 162.0, 161.5, 159.5, 153.2, 148.4, 132.4 (d, J = 4.5 Hz), 131.6, 129.2, 128.8 (d, J = 4.9 Hz), 128.4 (d, J = 3.5 Hz), 127.8, 123.1, 122.1, 120.0, 119.6, 119.4, 105.8, 64.6, 31.5. HR ESI-MS $(M + H)^+$ m/z = 546.9733 (Cacld for $C_{23}H_{16}BrFN_2O_4S_2$) 546.9741, HPLC purity: 98.1%.

4.6. Topo I-Mediated pBR322 DNA relaxation assay

The effects of QCs on DNA relaxation catalyzed by Topo I (TaKaRa, Kyoto, Japan) was evaluated by measuring the relaxation of pBR322 DNA (TaKaRa, Kyoto, Japan) by employing CPT as a standard. The assay was performed according to the manufacturer's instructions with

modification. The reaction mixture was incubated at 37 °C for 30 min. Then, it was terminated by the additional of dye solution (1% SDS, 0.02% bromophenol blue and 25% glycerol). The mixtures were applied to 1% agarose gel and subjected to electrophoresis for 1 h at 90 V, in TAE buffer (40 mM Tris-acetate, 2 mM EDTA). Gels were stained for 30 min in an aqueous solution of Ged Red (0.5 μg·mL^{-1}). DNA bands were visualized by transillumination with UV light and then photographed with an Alpha Innotech digital imaging system.

4.7. Animals

Male BALB/c mice (6–7 weeks old) were supplied from the Experimental Animal Centre of Guang Dong Province (approval documents: SCXK/20130002). The use of mice was reviewed and approved by the Ethics Committee for Animal Experimentation of the Guangdong University of Technology (Guangzhou, China) and was in accordance with the National Institutes of Health Guide for the Care and Use of Laboratory Animals (the 7th edition, USA).

4.8. Measurement of ear edema

Mice were randomly divided into difference groups. Control group, both ears of BALB/c mice were topically treated with 15 μL of acetone (vehicle) acetone 30 min prior to application of another acetone. Model group, both ears of BALB/c mice were topically treated with 15 μL of acetone 30 min prior to application of 0.08 nmol of TPA in 15 μL of acetone. Experiment groups, both ears of BALB/c mice were topically treated with CPT (2 μM) or QCs (4 μM) in 15 μL of acetone 30 min prior to application of 0.08 nmol of TPA in 15 μL of acetone. All mice were sacrificed 8 h after TPA (acetone for control group) treatment. Ear punches (5 mm in diameter) were taken immediately, weighed, frozen, and stored at −80 °C for next experiment.

4.9. Cell viability assay

Cell viability was assessed using a Cell Counting Kit-8 assay (CCK-8 from Dojindo, Kumamoto, Japan) according to the manufacturer's instructions. Briefly, cells were seeded in 96-well plates (1×10^4 cell per well) were stimulated with various concentration of **5i** and **5l** in the presence or absence of LPS (1 μg·mL^{-1}). CCK-8 was added to each well of the 96-well plates and incubated for 4 h, and the absorbance at 450 nm was measured using a microplate reader (Bio-Tek).

4.10. Measure of NO concentration

Briefly, the HaCaT cells (3×10^5 cell per well) were plate in 48-well plates over night. The cells were pretreated with CPT, **5i** and **5l** for 4 h and inflammation was stimulate with the addition of LPS (1 μg. mL^{-1}) for 20 h. Cell culture supernatants were collected and reacted with the Griess reagent in a 1:1 ratio, and the absorbance at 570 nm was measured using a microplate reader (Bio-Tek).

4.11. Development of IMQ-induced psoriasis-like mice model

One day before IMQ or vaseline treatment, mice were anesthetized by intraperitoneal injection of 50 mg/kg of sodium pentobarbital, their fur was shaved locally with an electric clipper. Mice received a daily topical dose of 62.5 mg of IMQ cream on the shaved dorsal skin for 7 consecutive days and the equivalent amount of petroleum jelly was applied to the control group. To examine the efficacy of QCs, mice were randomly divided into five groups (n = 6 per group): a vehicle-treated petroleum jelly-induced control group (abbreviated C), a vehicle treated IMQ-induced model group (IMQ), a CPT (5 mg/kg)-treated IMQ-induced group (CPT), and a **5i** and **5l** (50 mg/kg)-treated IMQ-induced group (**5i** and **5l**). The appropriate agents formulated in 200 μL of vehicle (consisting of 12% ethanol, 23% normal saline, 5% tween 80, and 60% peanut oil) were administered by oral gavage with a stomach-filling needle prior to application of 62.5 mg of IMQ cream, whereas the control and model groups received only 200 μL of vehicle. All groups' mice were sacrificed after 7 day, and the skins were collected for next experiments.

4.12. Histopathology and immunohistochemistry analyses

For H&E, the samples from different treatment groups were fixed in 10% formalin and embedded in paraffin for histological examinations. Sections of the ear or skin samples were cut and mounted on polylysin-coated slides. Each section was deparaffinized in xylene, rehydrated through a series of graded alcohols, and subjected to stain with hematoxylin and eosin. The thickness of the epidermis was measured using a Nikon light microscope (Japan) equipped with an ocular micrometer by the magnification (200×) in 15 fields per section. The number of dermal infiltrating inflammatory cells was determined by counting the stained cells at five different areas.

For immunohistochemistry staining, paraformaldehyde-fixed and paraffin-embedded ear or skin specimens were deparaffinized, antoclaved, heat-processed for antigen retrieval in citrate saline buffer, and incubated with purified rabbit anti-mouse COX-2, P65, IL-17A, IL-22, IL-23, TNF-α, or IFN-γ (abcam, UK) at 1:50 dilution overnight at 4 °C. All procedures were performed according to the manufacturers' guidelines.

4.13. Real-time polymerase chain reaction (RT-PCR)

Total RNA was extracted from collected cells or back skin on BALB/c by using trizol reagent. The synthesis of cDNA on 2 μg RNA was using the Revert Aid First Strand cDNA Synthesis Kit, and the expression of relative genes were measured with ABI Stepone plus Fast Real-Time PCR system by using a Fast Start Universal SYBR Green Master (Rox) (Roche Diagnostics, China). Primer sequences designed to detect the gene expression in mice were as follows: IL-17A, forward primer, 5′-TCA TGT GGT GGT CCA GCT TTC-3′, reverse primer, 5′-GAA GGC CCT CAG ACT ACC TCA A-3′, IL-22, forward primer, 5′-TTT CCT GAC CAA ACT CAG CA-3′, reverse primer, 5′-CTG GAT GTT CTG GTC GTC AC-3′, TNF-α, forward primer, 5′-TAT GGC CCA GAC CCT CAC A-3′, reverse primer, 5′-GGA GTA GAC AAG GTA CAA CCC ATC-3′, P65, forward primer, 5′-GTT TCG GGT AGG CAC AGC AAT-3′, reverse primer, 5′-TCG AGT CTC CAT GCA GCT ACG-3′, IL-23, forward primer, 5′-CTC ACC GTG ACG TTT AGG GA-3′, reverse primer, 5′-ACT AGA ACT CAG GCT GGG CAT C-3′, IFN-γ, forward primer, 5′-GTT GCT GAT GGC CTG ATT GTC-3′, reverse primer, 5′-CGG CAC AGT CAT TGA AAG CCT A-3′, GAPDH, forward primer, 5′-TGT GTC CGT CGT GGA TCT GA-3′, reverse primer, 5′-TTG CTG TTG AAG TCG CAG GAG-3′. The GAPDH gene was used as a reference to normalize the data that was quantitatively analyzed by using the $2^{-\Delta\Delta Cq}$ method.

Primers used for detecting the corresponding gene expression in HaCaT cell line: IL-6, forward primer, 5′-AGA GTA GTG AG GAA CAA GCC-3′, reverse primer, 5′-TAC ATT TGC CGA AGA GCC CT-3′, TNF-α, forward primer, 5′-TCC TTC AGA CAC CCT CAA CC-3′, reverse primer, 5′-AGG CCC CAG TTT GAA TTC TT-3′, IL-1β, forward, 5′-TGG AGA AGC TGT GGC AGC TAC CT-3′, reverse, 5′-GAA CGT CAC ACA CCA GCA GGT T-3′, IL-17A, forward, 5′-ACT ACA ACC GAT CCA CCT CAC-3′, reverse, 5′-ACT TTG CCT CCC AGA TCA CAG-3′. β-actin, forward primer, 5′-AGG GAA ATC GTG CGT GAC AT-3′, reverse primer, 5′-TCC TGC TTG CTG ATC CAC AT-3′, Cycle parameters were as follows: 95 °C for 10 min, 40 cycles of 95 °C for 15 sec, and 60 °C for 60 sec.

4.14. Western blot analysis

Back skins collected from BALB/c were kept in −80 °C and incubated in RIPA buffer on ice-bath for 30 min. The skin extractions were centrifuged at 12,000 rpm for 10 min at 4 °C. The supernatant was

collected and protein concentration was measured by BCA kit for protein quantification. Equivalent protein (40 μg) from each sample was load to SDS-PAGE and transferred to PVDF membrane. The PVDF membranes were blocked with 5% (w/v) BSA in TBST and incubated with anti-p65, anti-TNF-α, anti-IL-17A, anti-IL-22, anti-IL-23, and anti-IFN-γ and β-actin (Beyotime Biotechnology Co. Beijing China) over night at 4 °C, subsequently washed using TBST, probed with specific secondary antibodies coupled to HRP. An enhanced chemiluminescence method (ECL) was used to detect the immunoreactive protein by ECL reagents and the signal was recorded by FuJi medical X-ray film.

4.15. Statistical analysis

The means ± standard error of mean (SEM) and one-way ANOVA were applied to statistical analysis. Graph Pad Prism 5 software was used to analyze the experiments data and $p < 0.05$ was considered to be significance and produce the diagrams.

Conflict of interest

The authors declare no competing financial interest.

Acknowledgments

This work was supported by the National Science Foundation of China (grant number 21272043 for Z.-Y. D.).

Appendix A. Supplementary material

The QCs decreased weight in the TPA-stimulated mice ear punches, **5i** and **5l** arrested the body weight of mice induced by IMQ, the ^{1}H NMR and ^{13}C NMR spectrum of QCs. Supplementary data to this article can be found online at https://doi.org/10.1016/j.bioorg.2019.03.073.

References

[1] J.E. Gre, A.M. Goldmin, J.T. Elder, M.G. Lebwohl, D.D. Gladman, J.J. Wu, N.N. Mehta, A.Y. Finlay, A.B. Gottlieb, Psoriasis, Nat. Rev. Dis. Primers 2 (2016) 1–17.
[2] M.A. Lowes, A.M. Bowcock, J.G. Krueger, Pathogenesis and therapy of psoriasis, Nature 445 (2007) 866–873.
[3] F.O. Nestle, D.H. Kaplan, J. Barker, Psoriasis, N. Engl. J. Med. 361 (2009) 496–509.
[4] A.H. Møller, S. Erntoft, G.R. Vinding, G.B. Jemec, A systematic literature review to compare quality of life in psoriasis with other chronic diseases using EQ-5D-derived utility values, Patient Relat Outcome Meas. 6 (2015) 167–177.
[5] H.L. Ha, H. Wang, P. Pisitkun, J.C. Kim, I. Tassi, W. Tang, M.I. Morasso, M.C. Udey, U. Siebenlist, IL-17 drives psoriatic inflammation via distinct, target cell-specific mechanisms, Proc. Natl. Acad. Sci. 111 (2014) 3422–3431.
[6] R. Bissonnette, J. Fuentes-Duculan, S. Mashiko, X. Li, K.M. Bonifacio, I. Cueto, M. Suárez-Fariñas, C. Maari, C. Bolduc, S. Nigen, M. Sarfati, J.G. Krueger, Palmoplantar pustular psoriasis (PPPP) is characterized by activation of the IL-17A pathway, J. Dermatol. Sci 85 (2017) 20–26.
[7] I. Raphael, S. Nalawade, T.N. Eagar, T.G. Forsthuber, T cell subsets and their signature cytokines in autoimmune and inflammatory diseases, Cytokine 74 (2015) 5–17.
[8] A.L. Croxford, S. Karbach, F.C. Kurschus, S. Wörtge, A. Nikolaev, N. Yogev, S. Klebow, R. Schüler, S. Reissig, C. Piotrowski, E. Brylla, I. Bechmann, J. Scheller, S. Rose-John, F.T. Wunderlich, T. Munzel, E. von Stebut, A. Waisman, IL-6 regulates neutrophil microabscess formation in IL-17A-driven psoriasiform lesions, J. Invest. Dermatol. 134 (2014) 728–735.
[9] M.A. Lowes, M. Suárez-Fariñas, J.G. Krueger, Immunology of psoriasis, Annu. Rev. Immunol. 32 (2014) 227–255.
[10] J.B. Telliez, M.E. Dowty, L. Wang, J. Jussif, T. Lin, L. Li, E. Moy, P. Balbo, W. Li, Y.J. Zhao, K. Crouse, C. Dickinson, P. Symanowicz, M. Hegen, M.E. Banker, F. Vincent, R. Unwalla, S. Liang, A.M. Gilbert, M.F. Brown, M. Hayward, J. Montgomery, X. Yang, J. Bauman, J.I. Trujillo, A. Casimiro-Garcia, F.F. Vajdos, L. Leung, K.F. Geoghegan, A. Quazi, D.J. Xuan, L. Jones, E. Hett, K. Wright, J.D. Clark, A. Thorarensen, Discovery of a JAK3-selective inhibitor: functional differentiation of JAK3-selective inhibition over pan-JAK or JAK1-selective inhibition, ACS Chem. Biol. 11 (2016) 3442–3451.
[11] A.S. Dobry, C.P. Quesenberry, G.T. Ray, J.L. Geier, M.M. Asgari, Serious infections among a large cohort of subjects with systemically treated psoriasis, J. Am. Acad. Dermatol. 77 (2017) 838–844.
[12] T. Wong, L. Hsu, W. Liao, Phototherapy in psoriasis: a review of mechanisms of action, J. Cutan. Med. Surg. 17 (2013) 6–12.
[13] L. Puig, A. López-Ferrer, A. Laiz, Etanercept in the treatment of psoriatic arthritis, Actas. Dermosifiliogr. 106 (2015) 252–259.
[14] L. Puig, M. Augustin, A. Blauvelt, A.B. Gottlieb, R. Vender, N.J. Korman, D. Thaçi, Y. Zhao, I. Gilloteau, B. Sherif, N. Williams, A. Guana, M.G. Lebwohl, Effect of secukinumab on quality of life and psoriasis-related symptoms: a comparative analysis versus ustekinumab from the CLEAR 52-week study, J. Am. Acad. Dermatol. (2019), https://doi.org/10.1016/j.jaad.2017.10.025.
[15] A. Nast, A. Jacobs, S. Rosumeck, R.N. Werner, Efficacy and safety of systemic long-term treatments for moderate-to-severe psoriasis: a systematic review and meta-analysis, J. Invest. Dermatol. 135 (2015) 2641–2648.
[16] K.A. Whartenby, D. Small, P.A. Calabresi, FLT3 inhibitors for the treatment of autoimmune disease, Expert Opin. Invest. Drugs 17 (2008) 1685–1692.
[17] M.A. Sikma, E.M. van Maarseveen, E.A. van de Graaf, J.H. Kirkels, M.C. Verhaar, D.W. Donker, J. Kesecioglu, J. Meulenbelt, Pharmacokinetics and toxicity of tacrolimus early after heart and lung transplantation, Am. J. Transplant 15 (2015) 2301–2313.
[18] Y. Fujita, S. Shinkuma, T. Nomura, H. Shimizu, Safety of ustekinumab for the treatment of psoriasis vulgaris with myotonic dystrophy, Eur. J. Dermatol. 26 (2016) 187–188.
[19] D. Colombo, N. Cassano, G. Altomare, A. Giannetti, G.A. Vena, Psoriasis relapse evaluation with week-end cyclosporine a treatment: results of a randomized, double-blind, multicenter study, Int. J. Immunopathol. Pharmacol. 23 (2010) 1143–1152.
[20] G.B. Li, S. Ma, L.L. Yang, S. Ji, Z. Fang, G. Zhang, L.J. Wang, J.M. Zhong, Y. Xiong, J.H. Wang, S.Z. Huang, L.L. Li, R. Xiang, D.W. Niu, Y.C. Chen, S.Y. Yang, Drug discovery against psoriasis: identification of a new potent FMS like tyrosine kinase 3 (FLT3) inhibitor, 1–(4-((1H–Pyrazolo[3,4–d]pyrimidin-4-yl)oxy)-3-fluorophenyl)-3-(5–(tertbutyl)isoxazol-3-yl)urea, that showed potent activity in a psoriatic animal model, J. Med. Chem. 59 (2016) 8293–8305.
[21] S.M. Vos, E.M. Tretter, B.H. Schmidt, J.M. Berger, All tangled up: how cells direct, manage and exploit topoisomerse function, Nat. Rev. Mol. Cell Biol. 12 (2011) 827–841.
[22] Y. Pommier, Drugging topoisomerases: lessons and challenges, ACS Chem. Biol. 8 (2013) 82–95.
[23] J. Sun, J. Han, Q. Zhu, Z. Li, J. Hu, Camptothecin fails to induce apoptosis in tumor necrosis factor-alpha-treated HaCaT cells, Pharmacology 89 (2012) 58–63.
[24] X.B. Wang, L. Luo, J. Zeng, Clinical observation of 10-hydroxycamptothecin on treatment of psoriasis, J. Dermatol. Venereology 1 (2001) 30–31.
[25] X.R. Lin, D.I. Wilkinson, T. Huang, E.M. Farber, Experimental studies on topoisomerase inhibitor camptothecin as an antipsoriatic agent, Chin. Med. J. Engl. 112 (1999) 504–508.
[26] J.R. Lin, X.M. Liu, Y.M. Bao, S.C. Hou, L.J. An, X.R. Lin, Effects of isocamptothecin, a novel camptothecin analogue, on proliferation, apoptosis and telomerase activity in HaCaT cells, Exp. Dermatol. 17 (2008) 530–536.
[27] X. Liu, J. Lin, Y. Bao, X. Lin, L. An, Camptothecin-mediated apoptosis and anti-proliferation effect is accompanied by down-regulation of telomerase activity in HaCaT cells, J. Dermatol. Sci. 42 (2006) 262–264.
[28] A. Rialdi, L. Campisi, N. Zhao, I. Marazzi, Topoisomerase 1 inhibition suppresses inflammatory genes and protects from death by inflammation, Science 352 (2016), https://doi.org/10.1126/science. aad7993.
[29] L. van der Fits, S. Mourits, J.S. Voerman, M. Kant, L. Boon, J.D. Laman, F. Cornelissen, A.M. Mus, E. Florencia, E.P. Prens, E. Lubberts, Imiquimod-induced psoriasis-like skin inflammation in mice is mediated via the IL-23/IL-17 Axis, J. Immunol. 182 (2009) 5836–5845.
[30] N.H. Shear, J. Prinz, K. Papp, R.G. Langley, W.P. Gulliver, Targeting the interleukin-12/23 cytokine family in the treatment of psoriatic disease, J. Cutan. Med. Surg. 12 (2008) S1–S10.
[31] A.S. Lønnberg, C. Zachariae, L. Skov, Targeting of interleukin-17 in the treatment of psoriasis, Clin. Cosmet. Investig. Dermatol. 7 (2014) 251–259.
[32] A.B. Van Belle, M. de Heusch, M.M. Lemaire, E. Hendrickx, G. Warnier, K. Dunussi-Joannopoulos, L.A. Fouser, J.C. Renauld, L. Dumoutier, IL-22 is required for imiquimodinduced psoriasiform skin inflammation in mice, J. Immunol. 188 (2012) 462–469.
[33] B. Baragañ, N.R. Norcross, C. Wilson, A. Porzelle, I. Hallyburton, R. Grimaldi, M. Osuna-Cabello, S. Norval, J. Riley, L. Stojanovski, Discovery of a quinoline-4-carboxamide derivative with a novel mechanism of action, multistage antimalarial activity, and potent in vivo efficacy, J. Med. Chem. 59 (2016) 9672–9685.
[34] V. Sharma, D.K. Mehta, R. Das, Synthetic methods of quinoline derivatives as potent anticancer agents, Mini. Rev. Med. Chem. 17 (2017) 1557–1572.
[35] D.D. Subhedar, M.H. Shaikh, B.B. Shingate, L. Nawale, D. Sarkar, V.M. Khedkar, F.A. Kalam Khan, J.N. Sangshetti, Quinolidene-rhodanine conjugates: facile synthesis and biological evaluation, Eur. J. Med. Chem. 125 (2017) 385–399.
[36] Z.Q. Liu, S.T. Zhuo, J.H. Tan, T.M. Ou, D. Li, L.Q. Gu, Z.S. Huang, Facile syntheses of disubstituted bis(vinylquinolinium)-benzene derivatives as G-quadruplex DNA binders, Tetrahedron 69 (2013) 4922–4932.
[37] V. Ramesh, B.A. Rao, P. Sharma, B. Swarna, D. Thummuri, K. Srinivas, V.G.M. Naidu, V.J. Rao, Synthesis and biological evaluation of new rhodanine analogues bearing 2-chloroquinolin and benzo[*h*]quinolin scaffolds as anticancer agents, Eur. J. Med. Chem. 83 (2014) 569–580.
[38] P.H. Li, P. Zeng, S.B. Chen, P.F. Yao, Y.W. Mai, J.H. Tan, T.M. Ou, S.L. Huang, D. Li, L.Q. Gu, Z.S. Huang, Synthesis and mechanism studies of 1, 3-benzoazolyl substituted pyrrolo[2,3–*b*]pyrazine derivatives as nonintercalative topoisomerase II catalytic inhibitors, J. Med. Chem. 59 (2016) 238–252.
[39] X. Wu, M. Song, K. Rakariyatham, J.K. Zheng, M.Q. Wang, F. Xu, Z.L. Gao, H. Xiao, Inhibitory effects of 4′-demethylnobiletin, a metabolite of nobiletin, on 12–O–tetradecanoylphorbol-13-acetate (TPA)-induced inflammation in mice ears,

J. Agric. Food Chem. 63 (2015) 10921–10927.
[40] C.H. Hsu, Y.S. Ho, C.S. Lai, S.C. Hsieh, L.H. Chen, E. Lin, C.T. Ho, M.H. Pan, Hexahydro-β-acids potently inhibit 12–O–tetradecanoylphorbol 13-acetate-induced skin inflammation and tumor promotion in mice, J. Agric. Food Chem. 61 (2013) 11541–11549.
[41] K.A. Hollywood, C.L. Winder, W.B. Dunn, Y. Xu, D. Broadhurst, C.E.M. Griffiths, R. Goodacre, Exploring the mode of action of dithranol therapy for psoriasis: a metabolomic analysis using HaCaT cells, Mol. BioSyst. 11 (2015) 2198–2209.
[42] F. Shao, T. Tan, Y. Tan, Y. Sun, X.X. Wu, Q. Xu, Andrographolide alleviates imiquimod-induced psoriasis in mice via inducing autophagic proteolysis of MyD88, Biochem. Pharmacol. 115 (2016) 94–103.
[43] Y.P. Wu, X.Z. Chen, X.J. Ge, H.W. Xia, Y.X. Wang, S.Y. Su, W.T. Li, M.T. Wei, H. Zhang, L.T. Gou, J. Li, X. Jiang, J.L. Yang, Isoliquiritigenin prevents the progression of psoriasis-like symptoms by inhibiting NF-κB and proinflammatory cytokines, J. Mol. Med. 94 (2016) 195–206.
[44] S.Z. Chen, K.S. Han, H. Li, J.R. Cen, Y.F. Yang, H.Z. Wu, W. Qun, Isogarcinol extracted from *garcinia mangostana* L. ameliorates imiquimod-induced psoriasis-like skin lesions in mice, J. Agric. Food Chem. 65 (2017) 846–857.
[45] A.B. Van Belle, M. de Heusch, M.M. Lemaire, E. Hendrickx, G. Warnier, K. Dunussi-Joannopoulos, L.A. Fouser, J.C. Renauld, L. Dumoutier, IL-22 is required for imiquimod-induced psoriasiform skin inflammation in mice, J. Immunol. 188 (2012) 462–469.
[46] J.L. Harden, L.M. Johnson-Huang, M.F. Chamian, E. Lee, T. Pearce, C.L. Leonardi, A. Haider, M.A. Lowes, J.G. Krueger, Humanized anti-IFN-gamma (HuZAF) in the treatment of psoriasis, J. Allergy Clin. Immunol. 135 (2015) 553–556.